CHAPTER 4

RESULTS AND DISCUSSIONS

4.1 Introduction

This Chapter presents the results of the experimental work performed in this research study. The effects of different salient parameters such as extra water, curing time, and curing temperature, superplasticizer and concentration of sodium hydroxide on the fresh properties and compressive strength of fly ash-based SCGC are discussed. The various mechanical properties such as compressive strength, splitting tensile and flexural strength, modulus of elasticity, Poisson's ratio, and creep and drying shrinkage of SCGC are also discussed. In addition, the physical properties of concrete such as density and water absorption are presented in this chapter.

4.2 Fresh Properties of Fly ash-based SCGC

As discussed in section 2.10.1, SCC is described by three key characteristics such as filling ability (flowability), passing ability (likelihood of blocking at reinforcement) and resistance to segregation (stability). In this study, to characterize the fresh geopolymer concrete as self-compactable, for each mix, tests such as slump flow, T_{50cm} Slump flow, V-Funnel, L-Box and J-Ring were attempted for determining the key properties of SCC. All of these tests were performed by following The European guidelines for SCC [11, 92]. The results of the fresh properties of various SCGC mixtures accompanied by the minimum and maximum levels proposed by ERNARC [92] are given in Table 4.1.

The results of the quantitative measurements and visual observations showed that except for mixtures M_1, M_4, M_{11}, M_{12} and M_{13}, all the other concrete mixtures exhibi-

Table 4.1 Fresh Properties Test Results

Mix Code	Fresh properties				
	Slump flow diameter (mm)	$T_{50\ cm}$ Slump flow time (sec)	V-Funnel flow time (sec)	L-Box (H_2/H_1) Ratio	J-Ring blocking step (mm)
M_1	630	6.5	12.5	0.82	12
M_2	710	4.0	7	0.96	5
M_3	770	3.0	6	1.0	3
M_4	820	2.5	5.5	1.0	0
M_5	710	4.0	7	0.96	5
M_6	710	4.0	7	0.96	5
M_7	710	4.0	7	0.96	5
M_8	710	4.0	7	0.96	5
M_9	710	4.0	7	0.96	5
M_{10}	710	4.0	7	0.96	5
M_{11}	625	6.5	15.5	0.84	13
M_{12}	640	6.0	14	0.88	10
M_{13}	665	5.0	12.5	0.90	8
M_{14}	690	4.5	10	0.94	7
M_{15}	700	4.0	9.5	0.96	5
M_{16}	690	4.0	10	0.95	6
M_{17}	675	5.0	12	0.90	9
Acceptance Criteria for SCC as per EFNARC [92]					
Min.	650 mm	2 sec	6 sec	0.8	0 mm
Max.	800 mm	5 sec	12 sec	1.0	10 mm

ted adequate self-compacting characteristics either in terms of flowability (measured by the Slump-flow and V-Funnel tests) or passing ability (evaluated by the L-Box and J-Ring tests) and produced the desired results and satisfied the criteria to be classified as SCC. The fresh SCGC had enough deformability under its own weight and had quite a high viscosity, which is necessary to avoid segregation of coarse aggregate particles. The slump flow values of all produced concretes were in the range of 625-820 mm and the slump flow durations (T_{50cm} time) were less than 7 sec. The time measured via V-Funnel flow was in the range of 5.5-15.5 sec whilst the blocking ratio (H_2/H_1) ranged from 0.82 to 1.0 depending mainly on the water/geopolymer solids ratio, and the dosage of superplasticizer used in the concrete production. No specific segregation resistance test was carried out in the fresh state; however, the samples were checked for visual observations during the testing of fresh SCGC. The visual

examination of the final spread of the slump flow illustrated no signs of segregation (evidenced by a non-uniform coarse aggregate distribution) except for mixture M_4, which showed slight bleeding as well as segregation due to high amount of extra water.

4.3 Compressive Strength of Fly ash-based SCGC

Compressive strength is one of the most important mechanical properties of concrete and is considered as the characteristic material value for the classification of concrete. It is the most common measure used to evaluate the quality of hardened concrete. The compressive strength test results for all mix compositions are presented in Table 4.2. At the end of specified oven curing period, a set of three cubes for each test variable was tested at the ages of 1, 3, 7, and 28 days. The reported compressive strength is the average strength of three specimens.

Table 4.2 Compressive Strength Test Results

Mix Code	Compressive Strength (MPa)			
	1-Day	3-Days	7-Days	28-Days
M_1	53.46	54.33	55.08	56.29
M_2	45.01	45.85	46.94	48.53
M_3	37.31	37.90	38.56	39.78
M_4	22.58	22.98	23.44	24.18
M_5	51.03	51.98	52.26	53.80
M_6	51.41	52.20	52.69	53.92
M_7	51.68	52.33	52.72	53.99
M_8	44.81	45.64	45.98	47.54
M_9	48.56	49.22	49.80	50.77
M_{10}	47.99	48.83	49.67	50.42
M_{11}	40.85	41.77	42.84	44.69
M_{12}	42.02	42.68	44.17	46.86
M_{13}	44.74	45.28	46.19	48.90
M_{14}	47.83	48.52	49.44	51.52
M_{15}	41.45	42.14	43.62	44.87
M_{16}	45.19	46.02	47.32	49.28
M_{17}	46.96	47.64	48.98	50.46

It can be seen that (Table 4.2) for all mix compositions, compressive strength increased with concrete age. However, thereafter 1-day, there was little difference in the strength developed for all mixtures. The highest 28-days compressive strength (56.29 MPa) was achieved for mix M_1 while the lowest compressive strength (24.18 MPa) was recorded for mix M_4. As observed from Tables 4.1 and 4.2, except of mixes M_1, M_3, M_4, M_{11}, M_{12} and M_{13}, all the other SCGC mixtures satisfied the self-compatibility criteria and achieved the targeted 28-days compressive strength of 40 MPa. Mixes M_2, M_5, M_6, M_7, M_8, M_9, M_{10}, M_{14}, M_{15}, M_{16}, and M_{17} are all suitable mixes, as they exhibited targeted compressive strengths and displayed required self-compacting characteristics. However, keeping in view the economy of mix, out of these mixes, Mix M_{16} was selected as the most suitable SCGC mix and was considered for further investigation.

4.4 Effect of Salient Parameters on Fresh Properties and Compressive Strength of SCGC

4.4.1 Effect of Extra water

Water content is a crucial synthesis parameter and plays important roles during dissolution, polycondensation and hardening stages of geopolymerization [1]. In Portland cement concrete, water in the mixture undergoes chemical reaction with the cement to produce paste that binds the aggregates together. The reaction mechanism in case of geopolymer concrete is however different from that of Portland cement concrete [1]. In geopolymer concrete, water only increases the fluidity of the paste and provides workability to the mixture. When water is included in the geopolymer mix, it is excluded from the reaction and fills in the alumino-silicate gel pores [142]. Once the water evaporates from these pores, the surface area of the gel structure increases and results a highly porous geopolymer paste, which eventually leads to a decrease in compressive strength of hardened concrete [17]. Therefore, water content in the synthesis of geopolymer-based materials must be optimized so that all the individual stages of the geopolymerization process to be affected positively, while at the same time the geopolymeric paste to retain its workability [143].

To establish the effect of extra water on fresh properties as well as on compressive strength of SCGC, four mixtures M_1, M_2, M_3 and M_4 (Table 3.8) with identical mix composition, but different amount of extra water ranging from 10 to 20% of the mass of fly ash were prepared. The dosage of superplasticizer to the mass of fly ash was kept 7% while the concentration of sodium hydroxide solution was held 12 M. The test specimens were cured in the oven at a temperature of 70ºC for a period of 24 hrs.

4.4.1.1 Effect of Extra water on Fresh properties

As expected, the addition of extra water improved the workability characteristics of freshly prepared SCGC mixtures; however, the addition of extra water beyond 15% resulted in some bleeding as well as segregation of fresh concrete mix. The test results (Table 4.1) showed that except for mixture M_1 (10% extra water) and M_4 (20% extra water), the other two SCGC mixtures exhibited good flowability and produced desired results. It was found that suitable range of extra water was in the range of 12 to 15%. Higher amount than this gave bit segregated mix while lower amount gave relatively dry mix. It was observed that at the lowest water content (10%), the fresh mix was relatively stiff and viscous with low workability. This is because the low water content in the synthesis caused insufficient wetting of fly ash particles affecting negatively the paste workability and making difficult to flow itself. The fresh mix became increasingly flowable as the amount of extra water in the mix increased. This was due to the fact that the excessive water content in the mix diluted the molar concentration of alkali activator in the solution, which caused reduction in the viscosity of the mix as well as slowed down the rate of geopolymerization, which in turn resulted in increased workability. The effect of different contents of extra water on the individual workability test results is discussed in the subsequent sections.

4.4.1.1.1 Slump Flow Test

This test judges the capability of concrete to deform under its own weight against the friction of the surface with no restraint present [107]. Slump flow values of 650 mm to 800 mm are typically required for a concrete to be self-compactable [92]. At slump

flow greater than 800 mm, the concrete might segregate, and at less than 600 mm, the concrete might have insufficient flow to pass through highly congested reinforcement. The results of Slump flow test for all the four mixes with different contents of extra water are shown in Figure 4.1. Test results indicate that, except for Mixes M_1 (10% extra water) and M_4 (20% extra water), slump flow for the other two mixes is within the EFNARC range of 650-800 mm [92]. A minimum slump flow value of 630 mm was achieved when 10% amount of extra water was added to the mix. An increase in the amount of extra water reduced the viscosity and stiffness of the paste and decreased the inter-particle friction among the solid particles by increasing the paste volume, which in turn resulted to an increase in the slump flow spread of concrete. A good flowability with increasing extra water content till 15% was observed, afterwards slump flow increased but with some bleeding and segregation. This is because the excess water though increased the deformability of concrete by lowering the inter-particle friction; however, it reduced the paste viscosity, causing bleeding and segregation. The aggregate distribution and mortar halo around the spread in the slump flow test indicate the extent of segregation within the concrete. Except for Mix M_4 (20% extra water), the presence of mortar halo around the concrete spread was not observed in all the other three mixes.

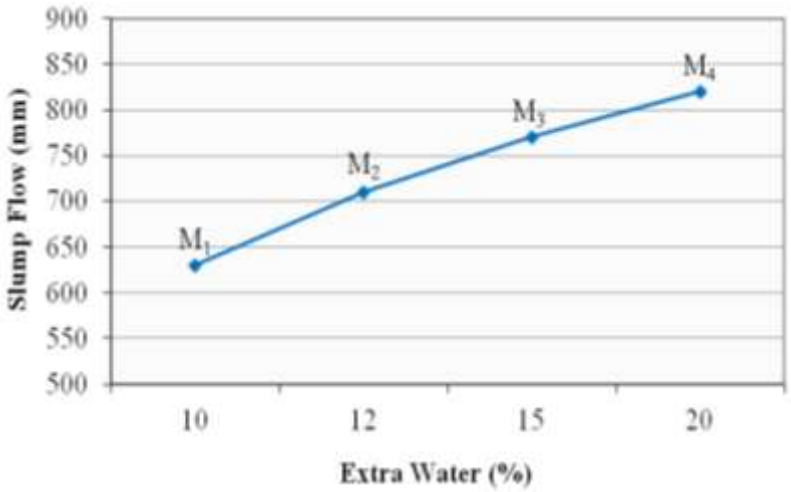

Figure 4.1 Effect of Extra water on Slump flow

4.4.1.1.2 $T_{50\ cm}$ Slump Flow Test

During the slump flow test, the time for concrete to reach 50 cm diameter ($T_{50\ cm}$ slump flow) is also measured. This $T_{50\ cm}$ flow time indirectly indicates the viscosity of concrete. Higher the flow time, higher the viscosity. The $T_{50\ cm}$ flow times for all mix compositions with different amounts of extra water are shown in Figure 4.2. Slump flow time less than 5 sec is recommended for a concrete to characterize as SCC [92]. Test results shows that $T_{50\ cm}$ slump flow varies between 2.5 and 6.5 sec. From the Figure 4.2, it can be seen that, except for Mix M_1 (10% extra water), all the other three SCGC mixes qualify the permissible limits of 2-5 sec given by EFNARC guidelines [92]. A maximum slump flow time of 6.5 sec was recorded for mix M_1 containing 10% of amount of extra water. An increase in the amount of extra water in the mix increased the fluidity and flowability of concrete by lowering the inter-particle friction and paste viscosity, which in turn resulted to a decrease in $T_{50\ cm}$ flow time.

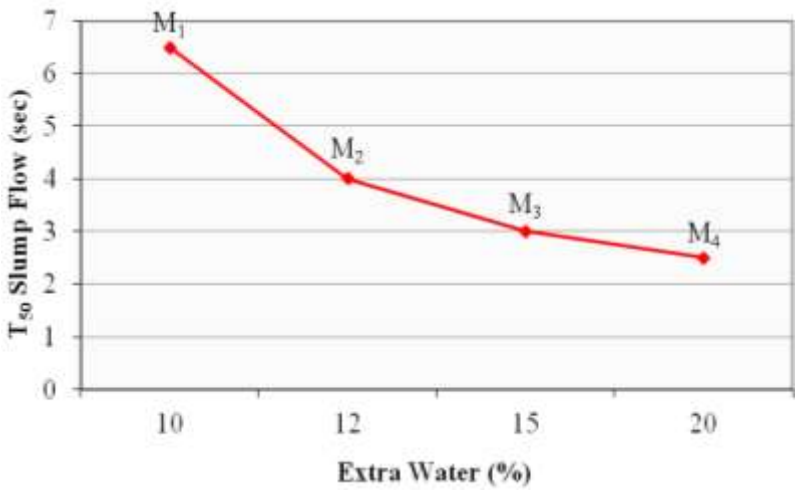

Figure 4.2 Effect of Extra water on T_{50} Slump flow

4.4.1.1.3 V-Funnel Test

V-Funnel test is primarily used to determine the filling ability (flowability) of concrete. This test suggests an opinion about the viscosity of concrete and measures the capability of concrete to pass through the confined spaces without segregation and blocking. To measure the filling ability and assess the stability and segregation

resistance of freshly prepared SCGC, all the four mixes with different amounts of extra water were tested by V-Funnel test. The V-Funnel flow time values obtained from the test are shown in Figure 4.3. As per EFNARC guidelines [92], flow time ranging from 6 sec to 12 sec is considered adequate for a concrete to be self-compactable. According to the results of test, the V-Funnel flow time varied between 5.5 and 12.5 sec. It can be seen that, except for mixture M_1 (10% extra water), all the other three concrete mixtures met the requirements of allowable flow time. A maximum flow time of 12.5 sec was recorded for the mix containing 10% of extra water indicating the lower filling ability and low deformability due to high paste viscosity and high inter-particle friction between the solid particles. With the increase in the amount of extra water, the inter-particle friction and the viscosity of the paste was reduced which in turn enhanced the ease of flow of concrete through the V-Funnel appratus. As a result, the V-Funnel flow time was decreased.

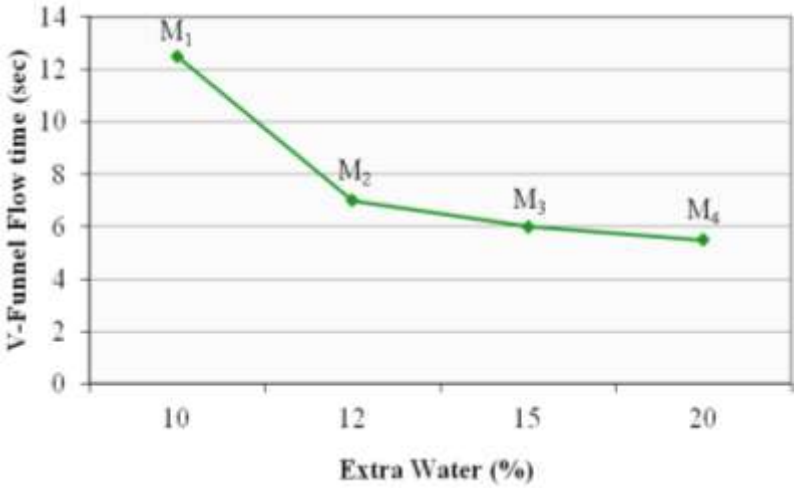

Figure 4.3 Effect of Extra water on V-Funnel flow time

4.4.1.1.4 L-Box Test

In this test, the ratio of heights (H_2/H_1) at the two edges of the horizontal section of L-Box is calculated which represents the filling and passing ability of SCC to flow through tight openings including spaces between reinforcing bars and other obstructions without segregation or blocking. The blocking ratio (H_2/H_1) of all the four SCGC mixes with different contents of extra water is shown in Figure 4.4.

According to EFNARC guidelines [92], the blocking ratio should be between 0.8 and 1.0. There is generally a blocking risk of the mixture when the blocking ratio is below 0.8. While assessing the fresh concrete for passing ability, it was observed that all the four SCGC mixes with different amounts of extra water passed through the bars of L-Box very easily and no blockage was seen in any of the mixes. The results of L-Box test show that, for all the four SCGC mixes, the blocking ratio (H_2/H_1) is above 0.8, which is as per EFNARC guidelines. A minimum blocking ratio value of 0.82 was recorded for the mix containing 10% of amount of extra water, which was still within the limits. A further increase in the amount of extra water in the mix reduced the paste viscosity and improved the fluidity and dispersal of the concrete which in turn produced the higher blocking ratio (H_2/H_1) value. For this reason, SCGC mixes containing 15% and 20% of extra water exhibited maximum value (1.0) of blocking ratio.

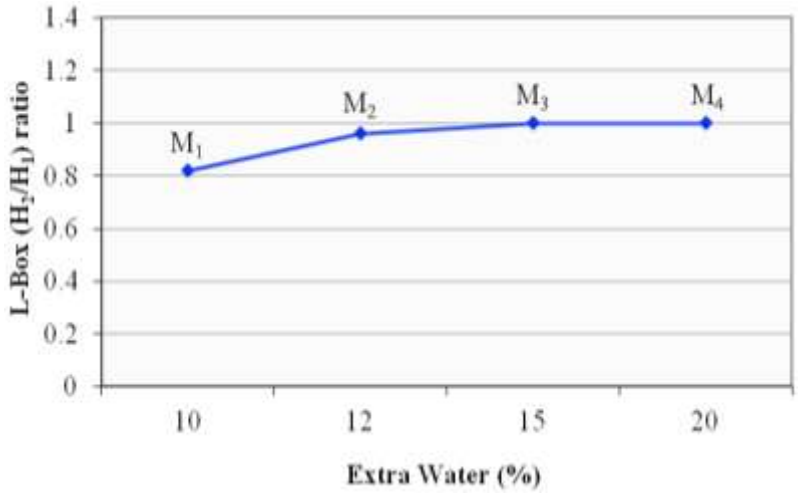

Figure 4.4 Effect of Extra water on L-Box (H_2/H_1) ratio

4.4.1.1.5 J-Ring Test

J-Ring test is used to measure the filling and passing ability of concrete by determining the degree to which the passage of concrete through the bars of the J-Ring apparatus is restricted. The J-Ring test was performed in conjunction with the slump flow test to assess the combined flowability and passing ability of SCGC. The difference in SCGC heights between inside and just outside the J-Ring (i.e. J-Ring

blocking step) was measured to investigate the extent to which the passage of SCGC through the vertical bars of the J-Ring was restricted. The J-Ring test results for the various SCGC mixes with different contents of extra water are shown in Figure 4.5. In general, greater J-Ring spread flow is associated with smaller values of blocking step, which represent higher passing ability. A blocking step value of maximum 10 mm has been recommended by EFNARC guidelines [92] for characterizing a concrete as SCC. As can be seen from the Figure 4.5, except for Mix M_1 (10% extra water), all the other three SCGC mixes were found to satisfy the requirements suggested by EFNARC and remained within the limits of 0-10 mm [92]. Similar to V-Funnel test results, an inverse relationship was obtained between the amount of extra water and the J-Ring blocking step value. At the lowest water content of 10%, the highest J-Ring blocking step value of 12 mm was achieved. With the increase in the amount of extra water in the SCGC mixes, the J-Ring blocking step value was decreased. This was due to the fact that as the amount of extra water was increased in the mix, the inter-particle friction and the viscosity of the paste were significantly reduced while the volume of the paste was increased. As a result, the aggregates were dispersed more efficiently and hence the concrete passed through the bars of the J-Ring with least congestion of the aggregates, consequently the blocking step value was reduced.

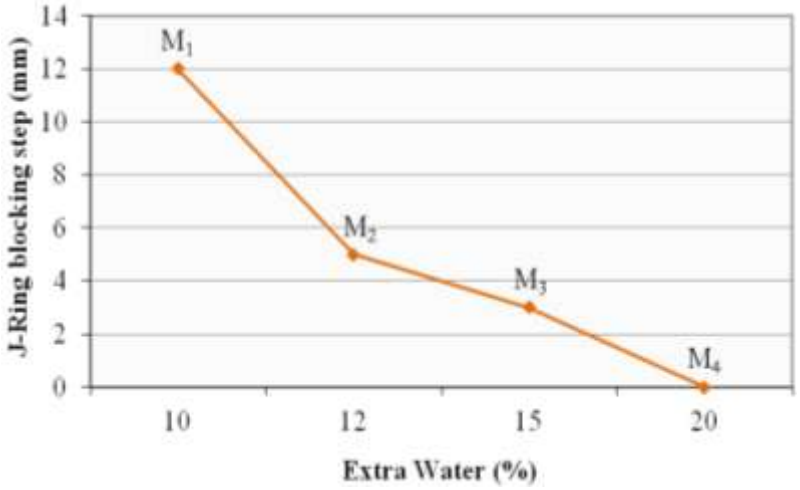

Figure 4.5 Effect of Extra water on J-Ring Blocking step value

4.4.1.2 Effect of Extra water on Compressive strength

Figure 4.6 illustrates the effect of extra water on the compressive strength of SCGC. In order to quantify the water content in the SCGC mix, the molar ratios of water/sodium oxide (H_2O/Na_2O) and the ratios of water/geopolymer solids by mass in different mix compositions were calculated. Each term was calculated from both solid and liquid parts of the mixture. For example, Na_2O was obtained from fly ash, sodium silicate and sodium hydroxide solution. Thus, for a given SCGC mixture, the moles of H_2O and Na_2O from fly ash, sodium silicate solution and sodium hydroxide solution were added together and the molar ratio of H_2O/Na_2O was obtained. Similarly, the total mass of water in the concrete mix was calculated by adding the masses of water in the sodium hydroxide solution, sodium silicate solution, and the extra water. The mass of the geopolymer solids was taken as the sum of the masses of fly ash, sodium hydroxide pellets, and the sodium silicate solids (i.e. the mass of SiO_2 and Na_2O in sodium silicate solution). The values of different molar ratios along with the compressive strength test results at various testing ages are presented in Table 4.3. The calculations of these ratios are given in Appendices B and C.

The results presented in Table 4.3 and Figure 4.6 indicated that the compressive strength of SCGC was very much affected by the extra water added into the mixture. The addition of extra water in the mix though improved the workability characteristics of fresh concrete, yet as expected it decreased the compressive strength of SCGC significantly. All the stages of geopolymerization process were negatively affected by increasing the water content in the aqueous phase of the synthesis and this is evident by the reduced compressive strengths shown in Table 4.3 and Figure 4.6. From the Figure 4.6, it can be seen that SCGC mix with amount of extra water of 10% shows the highest compressive strength at all testing ages compared to the mixes containing 12%, 15% and 20% of extra water. It is known that the H_2O/Na_2O molar ratio of the mix significantly influences the compressive strength of geopolymeric concrete. As this ratio increases, the amount of OH^- in the solution increases which causes high amount of porosity and tends to decrease the compressive strength of geopolymer concrete [144]. The results shown in Table 4.3 demonstrate that the compressive strength of SCGC was significantly decreased as the H_2O/Na_2O molar ratio of the mix increased. According to the results, the compressive strength of SCGC mix specimens

decreased almost linearly as the H_2O/Na_2O ratio was increased from 13.29 to 16.65. Molar ratio H_2O/Na_2O of 16.65 yielded lowest compressive strength of 24.2 MPa at 28 days. This is likely due to the increase in the porosity of concrete, which occurred due to the excessive amount of OH^- in the higher H_2O/Na_2O ratios and the evaporation of large amount of water (present inside the gel pores) during heat curing at elevated temperature resulting significant decrease in the compressive strength of SCGC. As in geopolymer concrete, unlike to OPC based concrete, water is not chemically combined to the network but acts only physically increasing the fluidity of concrete, and is expelled from the geopolymer matrix during the heat curing and further drying periods, causing discontinuous micro-pores within the matrix eventually lowering the compressive strength of concrete [1]. Furthermore, excessive water diluted the liquid component of the SCGC mix and decreased the alkali activator concentration (Na_2O/H_2O) in the aqueous phase (Table 4.3), which slowed down the reaction mechanism of the geopolymer. It is generally accepted that the compressive strength of geopolymer-based materials is linked to the degree of geopolymerization as higher the degree of geopolymerization in the geopolymeric system, higher the obtained compressive strength. The degree of geopolymerization is known to be significantly affected by the concentration of the sodium hydroxide solution. Lower concentration of sodium hydroxide in the aqueous phase reduces the dissolving ability of oxides and alumino- silicate phases in the solid raw material and decreases the inter-molecular bonding of the geopolymeric material, leading to reduction in the mechanical strength [52].

Table 4.3 Composition Characteristics and Compressive strengths of SCGC Mixes produced with Different Contents of Extra water

Mix Code	Extra water (%)	Molar Ratio				w/s* Ratio	Compressive Strength (MPa)			
		SiO_2/Al_2O_3	Na_2O/Al_2O_3	Na_2O/H_2O	H_2O/Na_2O		1-Day	3-Day	7-Day	28-Day
M_1	10	3.48	0.559	0.075	13.29	0.31	53.5	54.3	55.1	56.3
M_2	12	3.48	0.559	0.072	13.96	0.33	45.0	45.8	46.9	48.5
M_3	15	3.48	0.559	0.067	14.97	0.35	37.3	37.9	38.6	39.8
M_4	20	3.48	0.559	0.060	16.65	0.39	22.6	23.0	23.4	24.2

w/s* = water/geopolymer solids

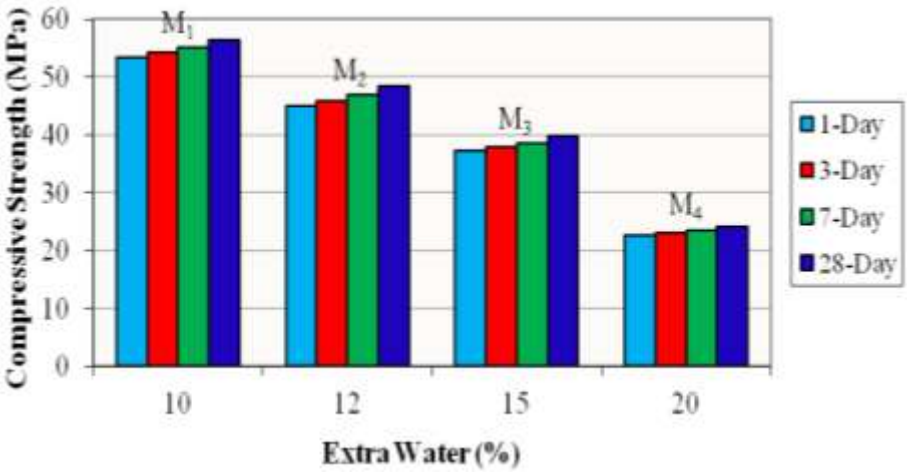

Figure 4.6 Effect of Extra water on Compressive strength

The effect of extra water is also illustrated in Figure 4.7 by plotting the compressive strength versus water/geopolymer solids ratio by mass. The test data shown in Figure 4.7 demonstrate that the compressive strength of the SCGC decreased as the ratio of water/geopolymer solids by mass increased giving rise to more free water in the mix leading to a more porous microstructure. As it is known that in geopolymer concrete, when high water content in the mix is used, it tends to produce large gel pores with water trapped inside and decreases the specific surface area of the concrete. Once the water is excluded from these pores, it results in a highly porous microstructure, which eventually results to a decrease in the compressive strength of concrete. On the other hand, when low water content in the mix is used, it limits the pore size in the geopolymer paste leading to an increase in the strength of geopolymer concrete [17].

From Figure 4.7, it can be seen that Mix M_1 with lower water/geopolymer solids ratio of 0.31 shows higher compressive strength values at all the ages compared to the Mixes M_2, M_3 and M_4 with water/geopolymer solids ratios of 0.33, 0.35 and 0.39 respectively. The compressive strength of SCGC decreases drastically as the water/geopolymer solids ratio increases. This shows that compressive strength of SCGC is inversely proportional to the water/geopolymer solids ratio. The trend of the results is similar to those observed by Hardjito et al. [63] for their tests on geopolymer concrete. Hardjito et al. [63] showed that the compressive strength of fly ash-based geopolymer concrete decreased as the ratio of water/geopolymer solids ratio by mass

increased. The trend is also somewhat similar to the well-known effect of water/cement ratio on the compressive strength of OPC concrete, although the mechanism of chemical reaction involved in the formation of the binders of two concretes is entirely different [1].

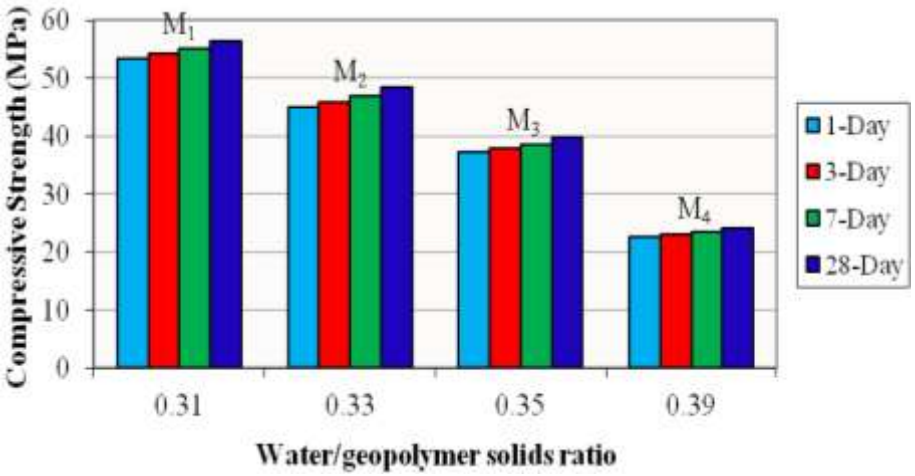

Figure 4.7 Effect of Water/Geopolymer solids Ratio on Compressive strength

4.4.2 Effect of Superplasticizer

Superplasticizer, also known as high-range water reducing admixture, is added to a concrete mixture to enhance the properties of concrete in both plastic and hardened state. Superplasticizer is an essential component of SCC to provide the necessary workability and to obtain a specified strength at lower cement content [11]. Superplasticizers perform their function by deflocculating the lumps of the binder particles. During the chemical interaction with binder and water, the negatively charged long molecules of superplasticizers dissolve in water to give ions with a very high negative charge (anions). These anions are absorbed onto the surface of the binder particles, wrap themselves around individual particles, and produce a negative surface charge on cement particles thus dispersing the particles by electrostatic repulsion, causing deflocculation. In doing so, water tied up within the original flocs is released which contributes to mobility of the paste and produces more fluid paste thus improving the workability of the concrete [27, 77]. When superplasticizers are used in concrete mixtures, some increase in compressive strength can also be anticipated. This might be due to the development of a uniform microstructure when

the cement is dispersed. The ability of superplasticizers to isolate cement grains provides an even distribution of cement particles throughout the paste and allows for a greater water exposure of each particle, which increases the early and long-term mechanical strength [37].

To study the effect of superplasticizer on the fresh properties as well as on the compressive strength of SCGC, mixtures M_5, M_{11}, M_{12}, M_{13} and M_{14} (Table 3.8) were prepared and tested. All the other test parameters were kept constant while the dosage of superplasticizer varied from 3 to 7% by mass of fly ash. The high dosages of superplasticizer (3 to 7%) were used considering the very stiff nature of geopolymer concrete and achieving the superior workability. The amount of extra water to the mass of fly ash and the concentration of sodium hydroxide solution were kept 12% and 12 M, respectively. The test specimens were cured in the oven at a temperature of 70ºC for a period of 48 hrs.

4.4.2.1 Effect of Superplasticizer on Fresh properties

The addition of superplasticizer was found to have positive influence on the properties of SCGC. The workability characteristics of freshly prepared SCGC were effectively improved with an increase in superplasticizer dosage. All mixtures showed almost good flowability and displayed good resistance to segregation. This is likely due to the fact that superplasticizers deflocculate the binder particles agglomerated together and release the water tied up in these agglomerations. The addition of superplasticizer in the SCGC mix adsorbed by coating the long molecules around the fly ash particles and imparted a highly negative charge. This in turn resulted in deflocculation and more effective dispersion of fly ash particles which contributed to mobility of the paste and improved the overall workability of SCGC. As indicated by the L-Box test results, all mixtures exhibited good passing ability and no blockage was seen in any of the mixes. The test data given in Table 4.1 demonstrate that superplasticizer dosage of up to 5% was found insufficient to produce the desired flowability and mixes were failed to exhibit the required workability characteristics for SCC. However, SCGC mixes containing superplasticizer dosage of 6% and 7% produced desired results and were within the EFNARC range [92] of SCC. The influence of different dosages of

superplasticizer on the individual workability test results is discussed in the following sections.

4.4.2.1.1 Slump Flow Test

The slump flow values for various SCGC mixes with different contents of superplasticizer are presented in Figure 4.8. The mixtures having flow diameter between 650 and 800 m have been accepted as appropriate in slump flow test [92]. It can be seen from the Figure 4.8 that all the mixtures except mixtures M_{11} (3% superplasticizer) and M_{12} (4% superplasticizer) fall into this category. Test results show that flow diameter increased with the increase in the quantity of superplasticizer. Since the water content for the all mixes was kept constant, an increment in superplasticizer content increased the fly ash dispersion in geopolymer matrix and facilitated the release of water tied up within the flocs, thus increasing the fluidity and flowability of the fresh mix, which in turn resulted to an increase in the flow diameter. For all five mixes, the slump flow diameter was between 625 and 710 mm, which is an indication of good deformability. The lowest flow diameter (625 mm) was measured for mixture containing 3% of superplasticizer whereas the highest flow diameter (710 mm) was measured for mixture containing 7% of superplasticizer.

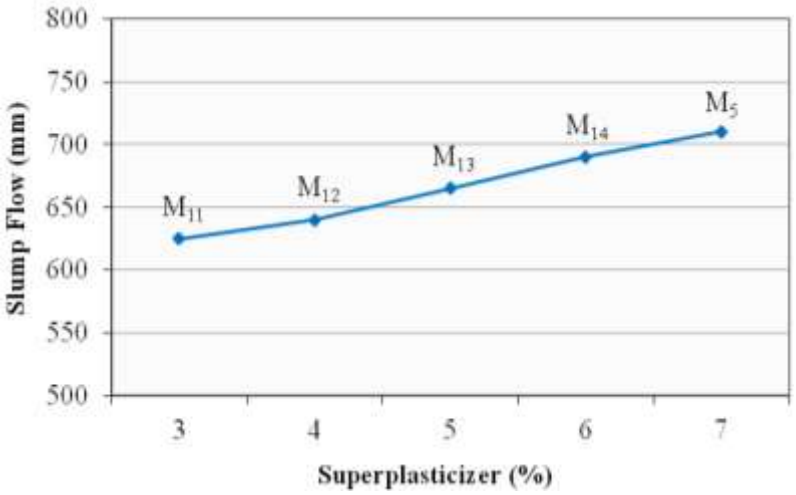

Figure 4.8 Effect of Superplasticizer on Slump flow

4.4.2.1.2 $T_{50\,cm}$ Slump Flow Test

The influence of different contents of superplasticizer on the $T_{50\ cm}$ flow time is demonstrated in Figure 4.9. Similar to slump flow test results, except for Mixes M_{11} (3% superplasticizer) and M_{12} (4% superplasticizer), all the other three SCGC mixes qualified the permissible limits of (2-5 sec) given by EFNARC [92]. Test results show that $T_{50\ cm}$ flow time varies between 4.0 and 6.5 sec. Concrete mix containing 3% of superplasticizer exhibited maximum flow time of 6.5 sec. With the increase in the quantity of superplasticizer, the flowability of the concrete was increased. As a result, the slump flow time was decreased.

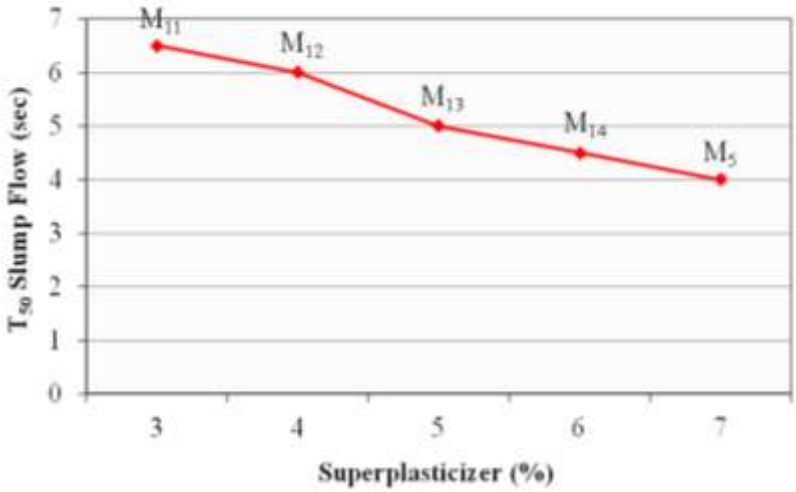

Figure 4.9 Effect of Superplasticizer on T_{50} Slump flow

4.4.2.1.3 V-Funnel Test

The effect of superplasticizer addition on the V-Funnel flow times is given in Figure 4.10. According to the results of test, the V-Funnel flow time varies between 7 and 15.5 sec. The highest flow time of 15.5 sec was measured for mixture containing 3% superplasticizer. Observation showed that the time taken for SCGC to flow through tapered section of V-Funnel was decreased as the superplasticizer content in the mix was increased. SCGC mixture containing 7% of superplasticizer displayed the lowest flow time of 7 sec. V-Funnel flow time values are acceptable till 6% of superplasticizer content as compared to the values between 6 and 12 sec suggested by EFNARC [92], but the minimum time is obtained for 7% of superplasticizer content.

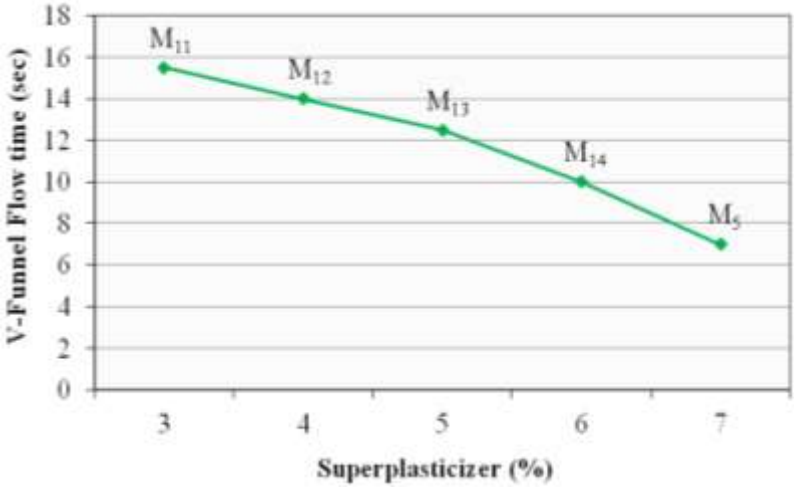

Figure 4.10 Effect of Superplasticizer on V-Funnel flow time

4.4.2.1.4 L-Box Test

The blocking ratio (H_2/H_1) of various SCGC mixes produced with different dosages of superplasticizer is shown in Figure 4.11. According to the results of L-Box test, the blocking ratio (H_2/H_1) varies between 0.84 and 0.96. For all the five mixes, the blocking ratio (H_2/H_1) is above 0.8 which is as per EFNARC guidelines [92]. A minimum value of 0.84 was measured for the mix containing 3% superplasticizer. Similar to extra water, a gradual increase in the value of blocking ratio (H_2/H_1) was observed with an increase in the dosage of superplasticizer. Superplasticizer dosage of 7% produced maximum value of 0.96 of blocking ratio.

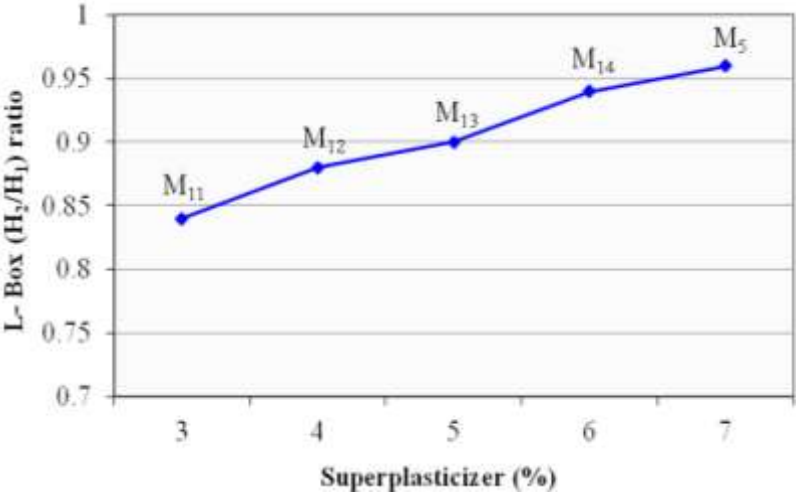

Figure 4.11 Effect of Superplasticizer on L-Box (H_2/H_1) ratio

4.4.2.1.5 J-Ring Test

The effect of superplasticizer content on the J-Ring test is depicted in the Figure 4.12. All the five mixes exhibited good passing ability, in that the J-Ring blocking step values for all the mixes were in the range of 0-10 mm except for the mix M_{11} (3% superplasticizer) where a J-Ring value of 13 mm was obtained. The J-Ring value is at its minimum for 7% of superplasticizer content and is still acceptable for 4% of superplasticizer. With the increase in the quantity of superplasticizer, the passing ability of concrete was increased. As a result, the J-Ring value of concrete was decreased.

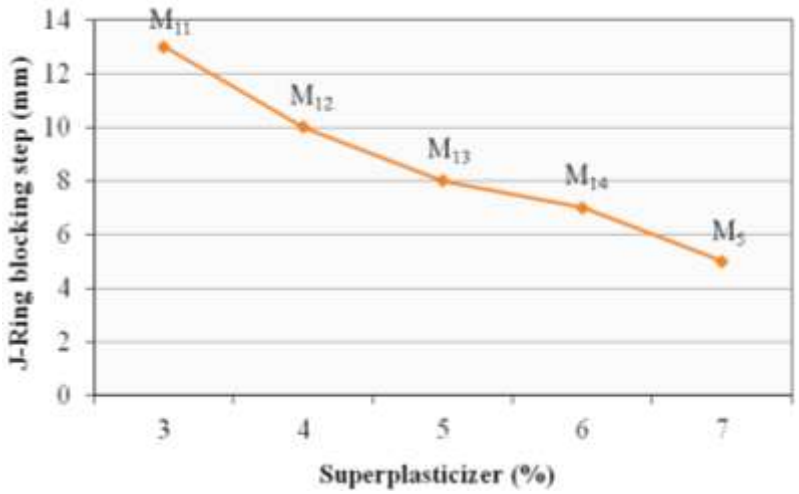

Figure 4.12 Effect of Superplasticizer on J-Ring Blocking step value

4.4.2.2 Effect of Superplasticizer on Compressive strength

Addition of superplasticizer in SCGC mix not only improved the workability characteristics of fresh concrete but also increased the compressive strength of the hardened concrete. Figure 4.13 demonstrates the effect of superplasticizer content on the compressive strength of SCGC. The test results shown in Figure 4.13 indicate that superplasticizer dosage of 3% exhibits the lowest compressive strength for all ages. This may be due to the incomplete packing of unreacted fly ash particles in the transition between the aggregate and geopolymer paste that occurred due to incomplete dissolution of large portion of fly ash particles leading to a less denser and homogenous microstructure eventually resulting the lower compressive strength of

SCGC. Figure 4.13 shows that as the amount of superplasticizer in the mix increases, the compressive strength also increases. SCGC mix specimens containing 7% of superplasticizer shows the highest compressive strength at all ages compared to the mixes containing 3%, 4%, 5% and 6% of superplasticizer. This is likely due to the improvement of pore structure of the hardened concrete leading to a more denser structure as the inclusion of superplasticizer in the mix leads to a reduction in the total pore volume and to a refinement of the pore structure [145]. Furthermore, the higher content of superplasticizer in the mix offered more effective action of dispersion, which resulted uniform distribution of fly ash particles in the mix, improved the homogeneity, and enhanced the bond strength between geopolymer paste and aggregates, consequently higher compressive strength was achieved. From the test results, it can also be seen that mix specimens with superplasticizer dosage of 7% produced slightly higher values of compressive strength than the mix containing 6% of superplasticizer. Compressive strengths of 51.5 MPa and 53.8 MPa were achieved for 6% and 7% superplasticizer at 28 days respectively, which shows no significant difference in terms of compressive strength. Reduction of superplasticizer dosage by 1% is very important for bulk quantity production as far as economy is concerned. As 6% of superplasticizer displayed the satisfactory results in terms of workability and achieved the targeted compressive strength, hence superplasticizer dosage of 6% was taken as the optimum and was used in further investigations.

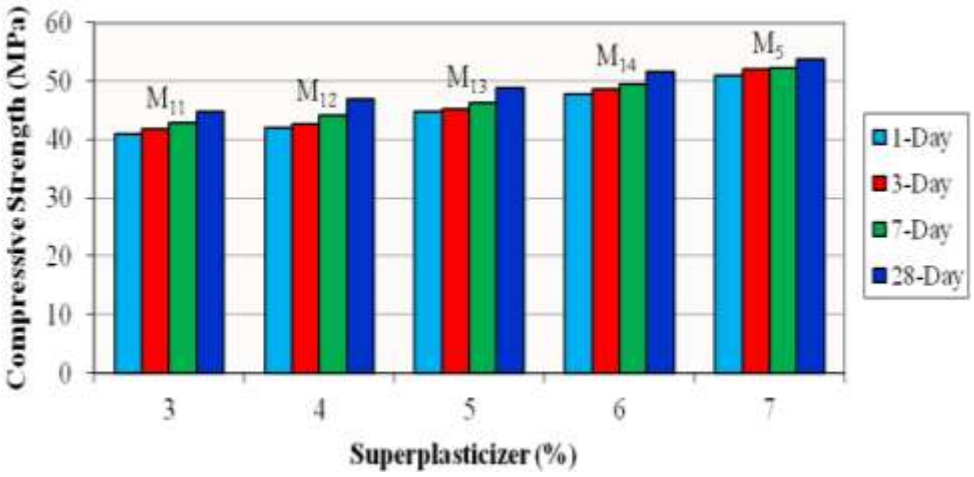

Figure 4.13 Effect of Superplasticizer on Compressive strength

4.4.3 Effect of Sodium hydroxide Concentration

Concentration of sodium hydroxide is the most important factor for geopolymer synthesis and significantly affects both the compressive strength and microstructure of geopolymers [54]. Sodium hydroxide concentration in the aqueous phase of the geopolymeric system acts on the dissolution process, as well as on the bonding of solid particles in the final structure. A higher concentration of sodium hydroxide increases the solubility of fly ash particles and enhances the process of Si and/or Si-Al oligomers formation leading to improved geopolymerization process, which eventually increases the compressive strength of geopolymer concrete. However, extremely high sodium hydroxide concentrations inhibit the geopolymerization process, resulting to a decrease in mechanical strength [146].

To study the effect of sodium hydroxide concentration on the fresh properties as well as on compressive strength of SCGC, four concrete mixtures M_{15} (8 M), M_{16} (10 M), M_{14} (12 M) and M_{17} (14 M) were prepared. All the other test parameters were kept constant. The details of the mix proportions are given in Table 3.8. To obtain the required workability characteristics of SCGC, a water content of 12% and superplasticizer dosage of 6% by mass of the fly ash were used in all the mixes.

4.4.3.1 Effect of Sodium hydroxide Concentration on Fresh properties

The results of fresh properties of various SCGC mixes containing different proportions of sodium hydroxide are presented in Table 4.1. Test results showed that concentration variation in sodium hydroxide between 8 M to 14 M had least effect on the fresh properties of SCGC. An increase in the concentration of sodium hydroxide decreased the amount of water required to prepare the sodium hydroxide solution, which increased the viscosity of the solution and enhanced the stiffness of the fresh mix. It was observed that concrete mixes containing higher contents of sodium hydroxide were more cohesive and fluidity and flowability of the SCGC mixes was reduced when the proportion of sodium hydroxide was increased. Test results (Table 4.1) indicated that the fresh properties of SCGC were slightly reduced as the concentration of sodium hydroxide was increased from 8 M to 14 M. This follows the

pattern reported in literature [147]. Siva et al. [147] found that the workability of low-calcium fly ash-based geopolymer concrete was decreased when the concentration of sodium hydroxide was increased from 10 M to 16 M. The effect of different sodium hydroxide concentrations on the individual workability test results is conferred in the succeeding sections.

4.4.3.1.1 Slump Flow Test

The effects of different concentrations of sodium hydroxide on slump flow test are shown in Figure 4.14. All the four mixes exhibited high flowability and displayed good resistance to segregation. The test results shown in Figure 4.14 indicate that the slump flow for all the mixes was within the EFNARC range of 650-800 mm [92]. A maximum slump flow value of 700 mm was achieved for a mix having sodium hydroxide concentration as 8 M. With the increase in concentration of sodium hydroxide between 8 M to 14 M, the slump flow diameter was reduced. This was due to the increase in the sodium hydroxide pellets that lowered the amount of water required to prepare the sodium hydroxide solution. As a result, the viscosity of the solution was increased and flow spread of the concrete was decreased.

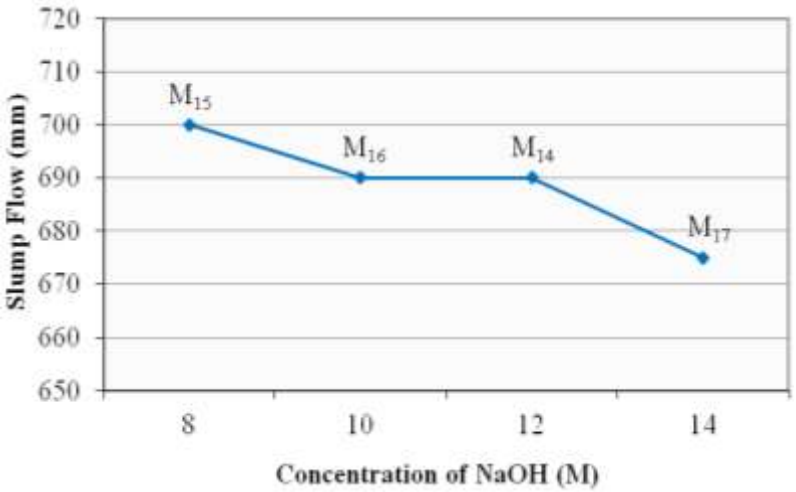

Figure 4.14 Effect of Sodium hydroxide Concentration on Slump flow

4.4.3.1.2 $T_{50\,cm}$ Slump Flow Test

Figure 4.15 illustrates the effect of sodium hydroxide concentration on the $T_{50\ cm}$ slump flow. As can be seen from the Figure 4.15, all of the four SCGC mixtures showed required times for reaching 50 cm slump flow ($T_{50\ cm}$) values in the range of 2-5 sec. A lowest slump flow time of 4 sec was recorded for mixes containing sodium hydroxide concentraton as 8 and 10 M. An increase in the concentration of sodium hydroxide increased the viscosity of the solution and reduced the fluidity of concrete resulting to an increase in $T_{50\ cm}$ time.

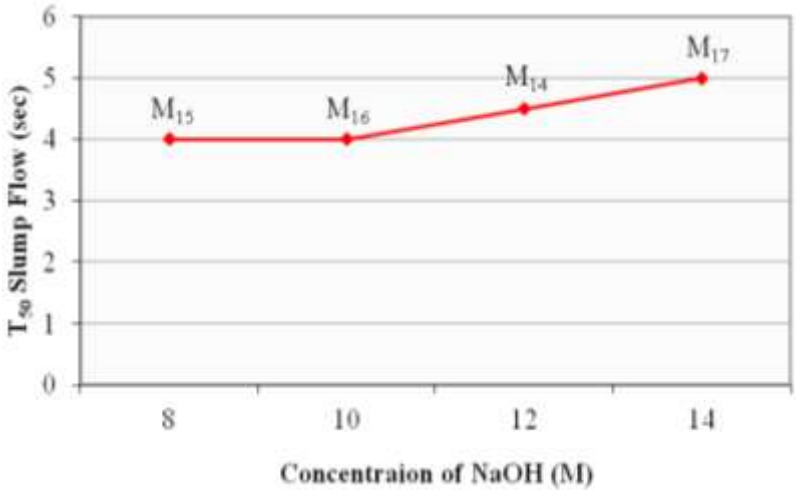

Figure 4.15 Effect of Sodium hydroxide Concentration on T_{50} Slump flow

4.4.3.1.3 V-Funnel Test

Figure 4.16 displays the influence of different concentrations of sodium hydroxide on the V-Funnel test. All the four SCGC mixes performed well in terms of stability as all mixes exhibited a V-Funnel flow time up to 12 sec. Though V-Funnel flow times for all the mixes were within the permissible limits given by EFNARC [92], most of the results remained towards the upper limit of 12 sec. A minimum flow time of 9.5 sec was recorded for mix with sodium hydroxide concentration as 8 M. An increase in the concentration of sodium hydroxide decreased the fluidity and filling ability of concrete, which in turn resulted to increase the V-Funnel flow time of the mix. SCGC mixture produced with 14 M sodium hydroxide concentration exhibited the maximum flow time of 12 sec.

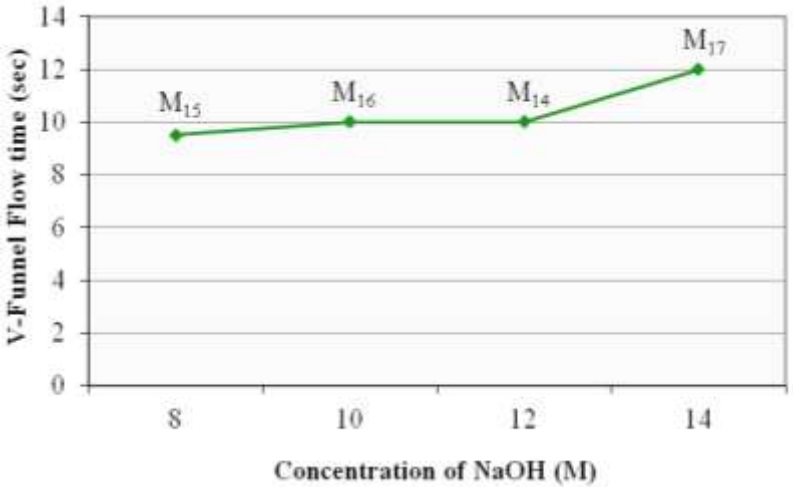

Figure 4.16 Effect of Sodium hydroxide Concentration on V-Funnel flow time

4.4.3.1.4 L-Box Test

Figure 4.17 shows the results of the L-Box test. Test results indicate that all the four mixes containing different concentrations of sodium hydroxide produced desired results and were within the EFNARC range of 0.8-1 [92]. The results of L-Box test show that the blocking ratio (H_2/H_1) of various SCGC mixes was in the range of 0.90-0.96. A maximum value of 0.96 was measured for the mix containing 8 M sodium hydroxide concentration. The blocking ratio (H_2/H_1) was gradually decreased with the increase in the concentration of sodium hydroxide. The same reasons and mechanism mentioned for slump flow and V-Funnel test results are commanding the explanations for the results of L-Box test.

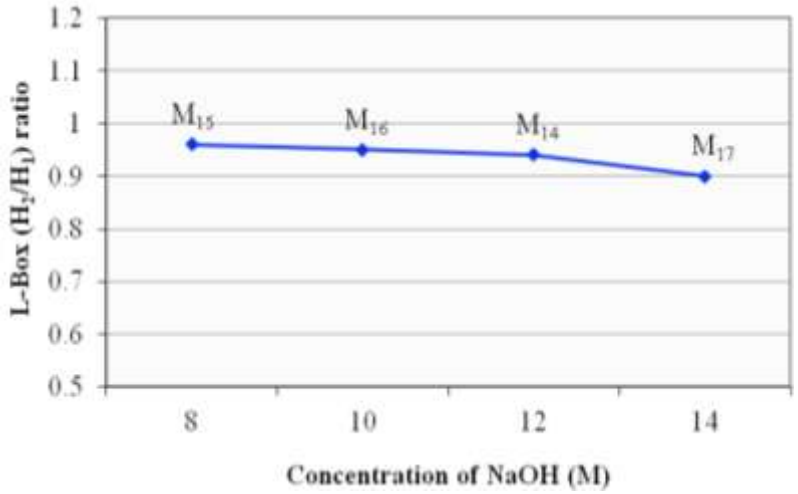

Figure 4.17 Effect of Sodium hydroxide Concentration on L-Box (H_2/H_1) ratio

4.4.3.1.5 J-Ring Test

Figure 4.18 demonstrates the results of the J-Ring test. The results of the quantitative measurements and visual observations showed that all the four mixes with different concentrations of sodium hydroxide had good passing ability and the J-Ring blocking step value for all the mixes was within the permissible limits of 0-10 mm given by EFNARC [92]. A lowest value of 5 mm was achieved for the mix containing 8 M sodium hydroxide concentration. With the increase in concentration of sodium hydroxide, the flowability and passing ability of fresh concrete was reduced. As a result, J-Ring blocking step value was also increased.

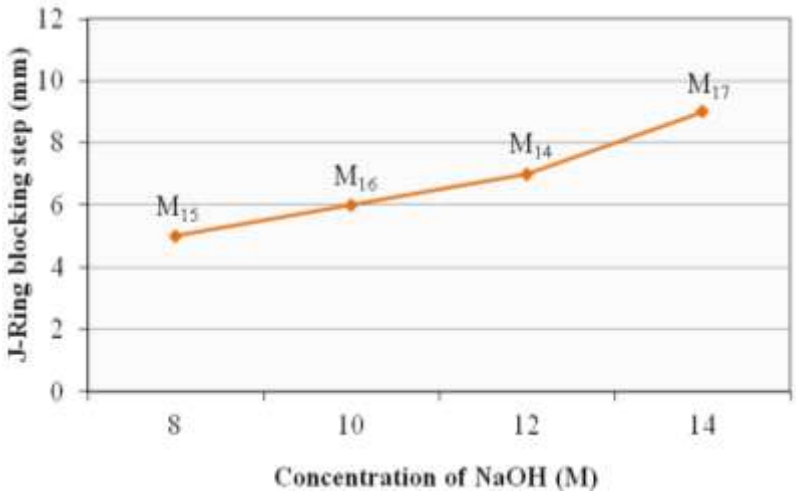

Figure 4.18 Effect of Sodium hydroxide Concentration on J-Ring Blocking step value

4.4.3.2 Effect of Sodium hydroxide Concentration on Compressive strength

Figure 4.19 illustrates the effect of sodium hydroxide concentration on the compressive strength of SCGC. The test results shown in Figure 4.19 demonstrate that the compressive strength of fly ash-based SCGC is not a monotonous function of sodium hydroxide concentration in the aqueous phase of the geopolymeric system. Under constant extra water content in the mix, the continuous addition of sodium hydroxide concentration in the aqueous phase caused positive as well as negative effects on the compressive strength of SCGC and this is evident from the results shown in Figure 4.19. Test results indicate that the compressive strength of fly ash-based SCGC increased as the sodium hydroxide concentration in the aqueous phase

increased from 8 M to 12 M; however, it decreased with further increase in sodium hydroxide concentration. This is because an increase in alkali concentration in the aqueous phase caused a substantial acceleration to the dissolution reactions thus improving the effectiveness of the geopolymerization process resulting to an increase in the compressive strength of SCGC. However, excessive hydroxide ion concentration caused alumino-silicate gel precipitation at the very early stages, and subsequent geopolymerization was hindered, resulting in lower compressive strength. It is generally accepted that the compressive strength of geopolymeric material is greatly dependent on the rate and extent of geopolymerization process, as higher the degree of geopolymerization, higher will be the obtained compressive strength. The geopolymerization process, which involves the dissolution of the source material species, transferring of the dissolved species from the solid surfaces to gel phase, and condensation of the gel phase, is significantly affected by the concentration of the sodium hydroxide solution [18, 52]. It is known that the dissolution rate of alumino-silicate oxides in the source material is directly related to the surface concentration of hydroxyl ions. Increasing sodium hydroxide concentration in the geopolymeric system, also increases the concentration of hydroxyl ions, which result in higher dissolution rates of Si and Si–Al phases of the source material, and improves the overall geopolymerization process. Considering this phenomenon, one would anticipate that the continuous increase of sodium hydroxide concentration in the aqueous phase of the geopolymeric system would affect positively on the compressive strength of the geopolymeric material. However, this is not in accordance with the experimental results shown in Figure 4.19. This is because although the formation of Si and/or Si-Al oligomeric precursors was enhanced due to increased dissolution rates caused by the increased contents of sodium hydroxide, was hindered under extremely high sodium hydroxide concentrations. At extremely high alkali concentrations, the species equilibrium shifts towards mononuclear species formation minimizing the concentration of oligomeric silicate species in the aqueous phase and thus, decelerating the process of geopolymerization [146]. In addition, when a too high concentration of sodium hydroxide is used, there is likely a formation of a relatively thin layer of the reaction products on the surface of fly ash particles. The sodium cations, which are normally presented at high concentrations in the geopolymeric systems, specifically adsorbed on the surface of fly ash particles consumes the surface

species, thus inhibiting the geopolymerization process. As a result, a reduction in mechanical strength is observed.

The experimental results presented here in Figure 4.19 are consistent with the prior observations made by other researchers [19, 148, 149]. Alonso and Palomo [148] found that when activator concentration increased above 10 M, a lower rate of polymer formation was produced resulting in the decrease of mechanical strength. Mustafa et al. [149], who investigated the effect of six different concentrations of sodium hydroxide ranging from 6 M to 16 M on the fly ash-based geopolymer paste, found that the specimens with sodium hydroxide concentration of 12 M showed highest compressive strength compared to the specimens produced with either of sodium hydroxide concentrations. Palomo et al. [19] also found that an activator with a 12 M of sodium hydroxide concentration led to better performances than 18 M of sodium hydroxide concentration. However, Hardjito et al. [51] found that alkaline concentration was proportionate to the compressive strength of geopolymer mortar. The authors revealed that higher concentration of sodium hydroxide solution resulted in a higher compressive strength of samples.

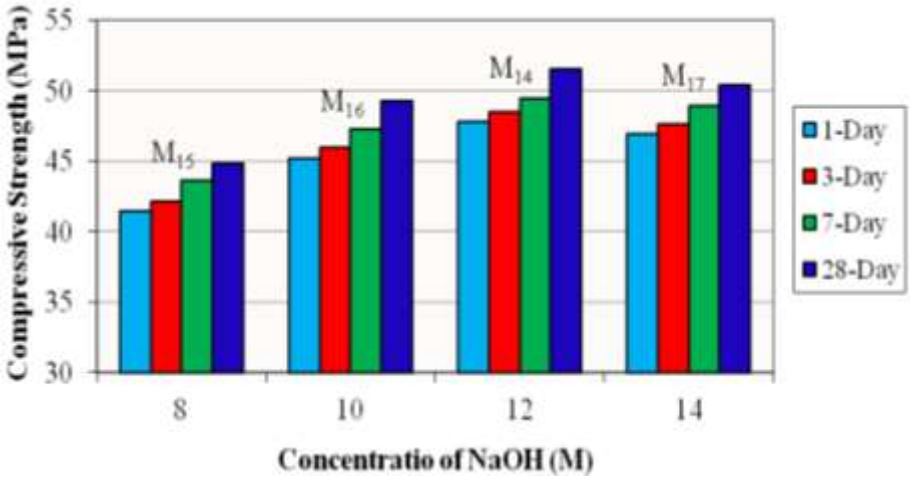

Figure 4.19 Effect of Sodium hydroxide Concentration on Compressive strength

The effect of sodium hydroxide concentration on the compressive strength of SCGC was also assessed in terms of alkali content in the mix, since, the concentration of sodium hydroxide (in terms of molar) does not reflect the effect of concentration of Na^+ ions in the mix especially when the activator contains the blend of sodium silicate and sodium hydroxide. Therefore, concentration of sodium hydroxide in terms of the

molar ratio of total Na_2O to Al_2O_3, SiO_2 and H_2O in the SCGC mixes was also calculated as the main indicator of the Na concentration in the mixes. Table 4.4 presents the molar ratios together with the obtained compressive strengths of the SCGC mixes at different testing ages. The calculation of these molar ratios is given in Appendix B.

Table 4.4 Composition Characteristics and Compressive strengths of SCGC Mixes produced with Different Sodium hydroxide Concentrations

Mix Code	NaOH Molar	Molar Ratio				*w/s ratio	Compressive Strength (MPa)			
		SiO_2/Al_2O_3	Na_2O/Al_2O_3	SiO_2/Na_2O	H_2O/Na_2O		1-Day	3-Day	7-Day	28-Day
M_{15}	8	3.48	0.47	7.41	17.24	0.35	41.4	42.1	43.6	44.9
M_{16}	10	3.48	0.51	6.78	15.47	0.34	45.2	46.0	47.3	49.3
M_{14}	12	3.48	0.56	6.23	13.96	0.33	47.8	48.5	49.4	51.5
M_{17}	14	3.48	0.60	5.78	12.69	0.32	47.0	47.6	49.0	50.5

*w/s = water/geopolymer solids

As can be seen from the data given in Table 4.4, the alkali content (Na_2O/Al_2O_3 molar ratio) played an important role in the compressive strength of SCGC and showed a positive effect on the compressive strength up to 0.56. The results indicate that the compressive strength of SCGC increased almost linearly when the alkali content (Na_2O/Al_2O_3 molar ratio) in the mix increased from 0.47 to 0.56, where it obtained its maximum value of 51.5 MPa at 28 days. After that, an increase in Na_2O/Al_2O_3 molar ratio resulting from the increase in sodium hydroxide concentration caused a decrease in the compressive strength of SCGC.

According to Steveson and Sagoe-Crentsil [150], the alkali concentration is a significant synthesis parameter and performs two roles in the geopolymeric system. Firstly, the hydroxide anion (OH^-) increases the solubility of the alumino-silicate species and secondly the sodium cation (Na^+) partially balances the charge of aluminates groups in the tectosilicate. Thus, a higher alkali content (Na_2O/Al_2O_3) would mean higher dissolution of fly ash particles and higher silicate and aluminate species ready for geopolymerization. Therefore, the increase of alkali content (Na_2O/Al_2O_3) of SCGC mix from 0.47 to 0.56 (caused by the addition of higher concentration of sodium hydroxide in the aqueous phase), resulted in formation of

more alumino-silicate gels and reduced the number and size of un-reacted fly ash particles in the geopolymer matrix consequently, increased the compressive strength of SCGC. Additionally, the decrease of the water content (H_2O/Na_2O) in the synthesis of SCGC (Table 4.4) due to increase in the sodium hydroxide concentration resulted in the increase of the initial Si concentration in the aqueous phase promoting in this way the formation of oligomers precursors, leading to an increase in the mechanical strength.

However, as shown in Table 4.4, the compressive strength of SCGC mix decreased as Na_2O/Al_2O_3 molar ratio increased from 0.56 to 0.60. This was due to the fact that as the concentration of sodium hydroxide in the mix increased, the SiO_2/Na_2O molar ratio decreased significantly (Table 4.4) causing a decrease in compressive strength. Lee and van Deventer [151] suggested that a high but appropriate soluble silicate is necessary for fly ash-based geopolymers as the presence of soluble silicate modifies the nature of reaction product and affects the degree of polymerization of the dissolved species in the alkaline solution. When the soluble silicate content is low enough, the dissolution of fly ash particles is inhibited resulting to reduction in mechanical strength. Therefore, it is necessary to add increased amounts of soluble silicate in the aqueous phase, so as the SiO_2/Na_2O ratio to be kept at high values and the polycondensation process to be promoted from the early stages of geopolymerization. Otherwise, too high concentrations of sodium hydroxide in the aqueous phase will cause negative effect on the geopolymerization process resulting decrease in the compressive strength [146]. As excess OH^- may result polycondensation reactions to occur not only at earlier but also much faster rate and therefore inhibit the dissolution of alumino-silicates, which needs enough time to proceed. Such a condition leads to the formation of a material with un-matured molecular structure caused by the incomplete dissolution of alumino-silicates and results relatively lower compressive strength [47].

It is of interest to note that although SCGC mix produced with 12 M sodium hydroxide concentration, provided the highest compressive strength, however, considering the economy of the mix, SCGC mix with sodium hydroxide concentration of 10 M was proposed as the most suitable mix. Since, the difference between the compressive strengths obtained with 10 M and 12 M concentrations was marginal. In

addition, SCGC mix produced with 10 M concentration displayed the satisfactory results in terms of workability and achieved the targeted compressive strength; hence, a sodium hydroxide concentration of 10 M was used in the later parts of the study.

4.4.4 Effect of Oven Curing Time

Curing of freshly prepared geopolymer concrete is the most crucial aspect and plays an important role in the geopolymerization process. Previous research has shown that both curing temperature and curing duration significantly influence the microstructural characteristics and mechanical strength development of geopolymer concrete. Higher curing temperature and extended curing time have been reported to result in higher compressive strength.

A wide range of heat curing durations and temperatures has been reported in literature for curing geopolymer-based concrete, ranging from room temperature to about 90°C and from 4 hrs to more than 24 hrs. To investigate the influence of heat curing duration on the compressive strength of fly ash-based SCGC, the test specimens with extra water of 12%, water/geopolymer solids ratio of 0.33, sodium hydroxide concentration of 12 M and superplasticizer dosage of 7% were cured in the oven at 70°C for different curing durations ranging from 24 hrs to 96 hrs. The effect of heat curing time on the compressive strength of SCGC is illustrated in Figure 4.20.

Figure 4.20 shows that SCGC mix specimens cured at 70°C for a period of 96 hrs exhibits the highest compressive strength for all testing ages. It can be seen that, the rate of increase in strength is rapid up to 48 hrs of curing time; after that, no appreciable increase in compressive strength. It is evident that compressive strength increases considerably with the increase in curing duration from 24 hrs to 48 hrs, however, when curing time further increases from 48 hrs to 96 hrs, no significant increase in compressive strength achieves. A strength of 53.80 MPa at 28 days is achieved with 48 hrs of heat curing. A little higher strength of 53.92 MPa is obtained with the 72 hrs of heat curing while strength of 53.99 MPa is achieved with 96 hrs heat curing.

The results shown in Figure 4.20 indicate that the compressive strength increases with increase in curing time. This is because longer curing time improves the geopolymerization process and results in the formation of more alkali aluminosilicate gel from the starting material, which in turn increases the compressive strength of geopolymer concrete [46]. However, curing at elevated temperature for extended periods of time resulted to have minimal effect on the compressive strength of SCGC. As, increasing the curing duration beyond 48 hrs does not show any significant gain in the compressive strength and a little increase in the compressive strength is observed when the curing time is increased from 48 hrs to 96 hrs. This is likely due to the initial heavy formation of the reaction product and a subsequent densification of material immediately upon alkaline introduction. The reaction product becomes exponentially less over time and the gain in strength occurs at a much slower rate as the time progresses [57]. The results shown in Figure 4.20 clearly demonstrate that longer curing time does not produce weaker material and results in lower strength as claimed by van Jaarsveld et al. [17]. The results of the test are in agreement with those observed by Hardjito et al. [63] in their study on fly ash-based geopolymer concrete.

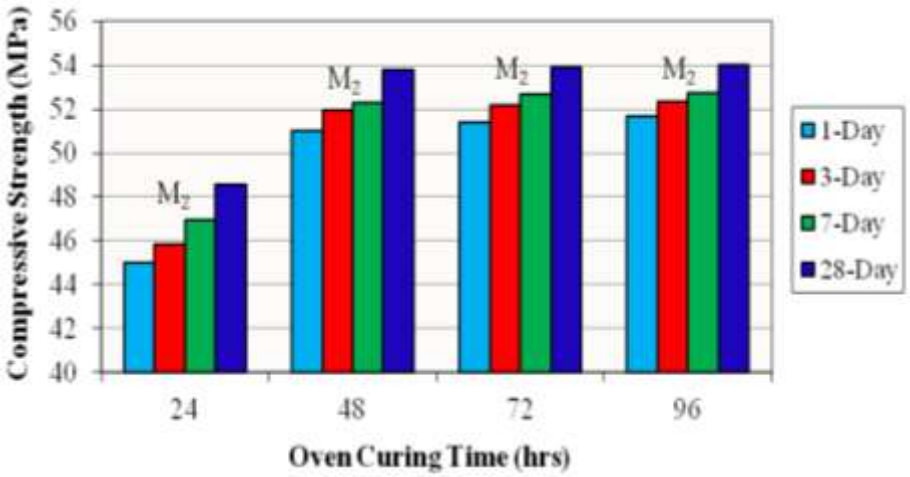

Figure 4.20 Effect of Curing Time on Compressive strength

4.4.5 Effect of Curing Temperature

Curing temperature plays significant role in the setting and hardening of the geopolymer concrete [51]. Generally, curing of fly ash-based geopolymer concrete is carried out at elevated temperatures. Higher temperatures activate alumino-silicate

phases in the fly ash and increase the rate of geopolymerization process, consequently accelerate the hardening of geopolymer concrete [17, 51]. However, elevated temperature during early stage of hardening process results to the formation of larger pores that may weaken the structure of geopolymer concrete, leading to a decrease in compressive strength [58].

As curing of fly ash-based geopolymer concrete is mostly carried out in the range of 60-90°C; therefore, in this series of tests, the curing temperature also varied from 60 to 90°C. Curing temperatures of 60°C, 70°C, 80°C and 90°C were used to assess the influence of curing temperature on the compressive strength development of SCGC. The test specimens with extra water of 12%, water/geopolymer solids ratio of 0.33, sodium hydroxide concentration of 12 M and superplasticizer dosage of 7% were cured in the oven for a period of 48 hrs. Figure 4.21 shows the effect of curing temperature on the compressive strength of SCGC.

Test results shown in Figure 4.21 indicate that higher curing temperature does not ensure higher compressive strengths as claimed by Hardjito et al. [46] in their study on fly ash-based geopolymer concrete. Test results show that an increase in the curing temperature from 60°C to 70°C increases the compressive strength of the concrete at all ages. However, increasing the curing temperature beyond 70°C decreases the compressive strength of SCGC. Xu and Deventer [25] revealed that for stable alkali reaction process of fly ash, a relatively higher temperature is required to accelerate the hydrothermal synthesis reaction since low curing temperature in fly ash-based geopolymers leads to a slower reaction time and an insufficient alkali reaction process, which in turn result in a lower compressive strength. The rise in curing temperature enhances the dissolution rate of solid alumino-silicate material. In addition, the total pore volume, pore size and surface area are slightly increased. This in turn increases the rate of reaction consequently higher compressive strength is achieved [55]. It is believed that an increase in the curing temperature from 60°C to 70°C increased the rate and extent of reaction through an increase in the heat of reaction; consequently increased the compressive strength of SCGC. Increasing the temperature from 60°C to 70°C also gave rise to dissolution of fly ash particles, which further accelerated the polymerization process resulting to an increase in the strength.

However, an increment in the curing temperature beyond 70°C caused a negative effect on the geopolymerization process, leading to a decrease in compressive strength of SCGC. This is because when the curing temperature was high enough, the specimens experienced a substantial loss of moisture. This was verified by examining the test samples visually at the time of testing. It was observed that the specimens with curing temperatures of 80°C and 90°C were relatively dry compared to the specimens cured at 60°C and 70°C. A possible explanation for this behaviour can be that when the samples were cured at temperatures higher than 70°C, the water remaining in the alumino-silicate gel pores was expelled more rapidly from hardened concrete. The spaces that were previously occupied by the water remained as micropores. These pores resulted in a microcrack path thus weakening the overall structure, which led to premature failure of concrete resulting in lower compressive strength. It is worth to mention that the removal of all structural water from geopolymer concrete is not beneficial, as geopolymerization requires the presence of moisture to maintain structural integrity and to achieve a good compressive strength [49].

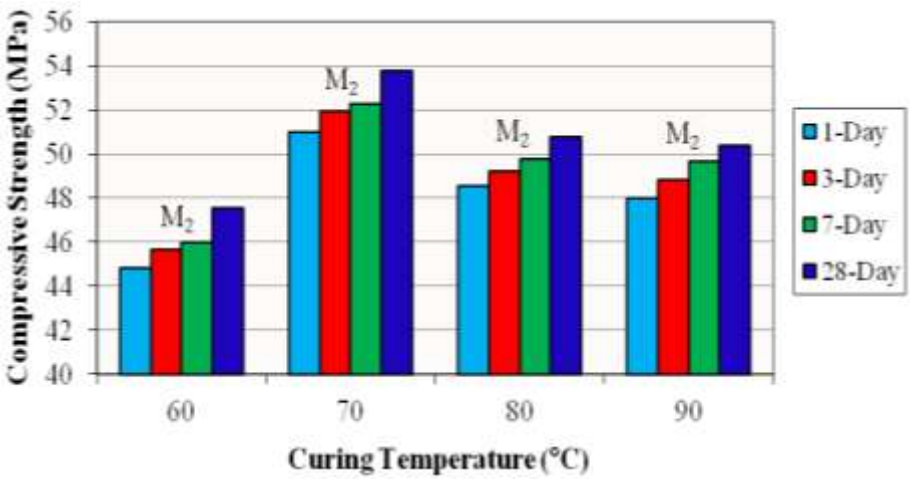

Figure 4.21 Effect of Curing Temperature on Compressive strength

4.5 Physical and Mechanical Properties of Selected SCGC and OPC Control Mixes

4.5.1 Physical Properties

4.5.1.1 Density

Density is the physical property of the material that measures the quantity of a substance per unit of space. The density of SCGC and OPC mix concrete was determined by dividing the weight of each specimen to its volume. The densities of both SCGC and OPC mix specimens after removing them from their moulds are presented in Table 4.5 and Figure 4.22. From test results, it can be seen that the density of selected SCGC mix ranges from 2295 to 2372 kg/m^3 while the density of reference OPC mix ranges from 2337 to 2397 kg/m^3. On average, the density of SCGC is 2332 kg/m^3, which is well within the range of 2240-2400 kg/m^3 prescribed for normal weight Portland cement concrete. Although the mix ingredients and proportions of SCGC were different from those of OPC control mix, the density values of SCGC are comparable to those of control OPC mix, indicating the good self-compaction of SCGC.

Table 4.5 Densities of SCGC and OPC Mix Specimens

Specimen No.	SCGC Mix			OPC Control Mix		
	Weight (kg)	Volume (m^3)	Density (kg/m^3)	Weight (kg)	Volume (m^3)	Density (kg/m^3)
1	2.315	0.001	2315	2.344	0.001	2344
2	2.355	0.001	2355	2.373	0.001	2373
3	2.295	0.001	2295	2.397	0.001	2397
4	2.372	0.001	2372	2.360	0.001	2360
5	2.348	0.001	2348	2.367	0.001	2367
6	2.339	0.001	2339	2.386	0.001	2386
7	3.652	0.00157	2326	3.669	0.00157	2337
8	3.619	0.00157	2305	3.714	0.00157	2366
9	3.647	0.00157	2323	3.681	0.00157	2345
10	3.676	0.00157	2341	3.730	0.00157	2376
11	3.668	0.00157	2336	3.723	0.00157	2371
12	3.655	0.00157	2328	3.696	0.00157	2354
Average			2332			2365

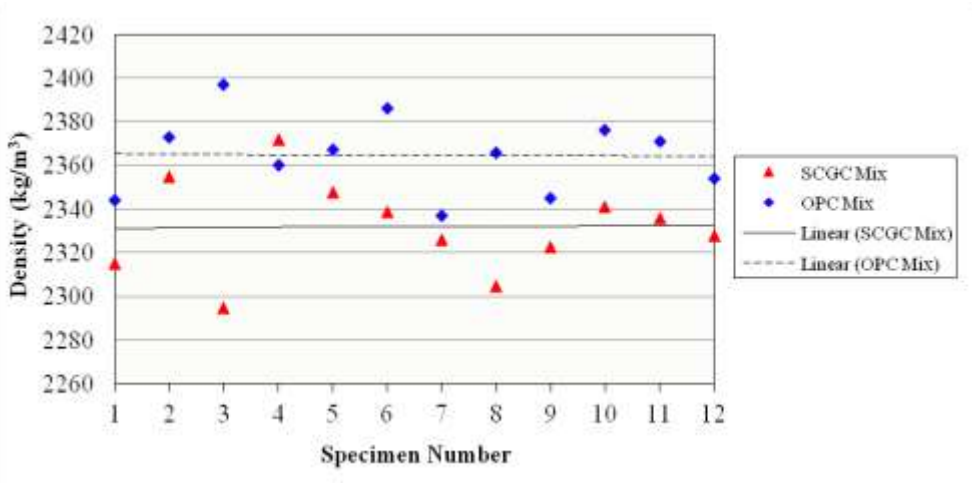

Figure 4.22 Densities of SCGC and OPC Mix Specimens

4.5.1.2 Water Absorption

Absorption is a process by which a liquid gets into and tends to fill the open pores in a porous solid body. The rate at which a dry concrete surface absorbs a liquid can be taken as a predictor of the durability of concrete. Water is one of the medium with which the concrete comes in contact. Hence, water absorption is widely used to indicate the absorptivity of concrete. It can be determined based on the increase in mass of a concrete specimen due to the penetration of water into its open pores.

Tables 4.6 through 4.9 present the results of water absorption test for the SCGC and the corresponding OPC control mix at the age of 28 days. Test results indicate that SCGC mix specimens displayed better performance with regard to water absorption. All of the SCGC mix specimens absorbed less water and produced lower absorption values than the OPC control mix specimens. From the test results, it can be seen that water absorption of SCGC mix specimens ranges from 2.73% to 2.95% whereas water absorption of OPC control mix ranges from 4.26% to 4.54%. On average, the water absorption of fly ash-based SCGC is 2.84%, which is relatively low compared to 4.41% of OPC mix. This is likely due to the less porous zone and very refined pore structure of SCGC compared to OPC control mix. In geopolymer-based concretes, the paste-aggregate interface has been reported to be highly dense and uniform, with only minimal differences between this region and the area of the matrix away from the aggregate particles. This differs from the microstructure

reported in OPC-based concrete, where the area between the paste and aggregates is the weakest part of the material and is characterized by a high porosity [152]. The low range of water absorption exhibited by SCGC mix specimens is an indication of limited pore connectivity and reduced open porosity of SCGC that inhibit the high flow of water into the concrete compared to the conventional Portland cement concrete. Olivia et al. [153] have reported similar trend of results. In a study on geopolymer concrete produced with low-calcium fly ash, Olivia et al. [153] revealed that geopolymer concrete showed low water absorption and sorptivity than the corresponding Portland cement concrete and found that the water absorption of fly ash-based geopolymer concrete was less than 5%, indicating good quality of concrete with regard to water absorption.

The absorption values of SCGC mix specimens are also compared with the recommendations given by Concrete Society Board, CEB-FIP [154]. Table 4.10 presents assessment criteria for absorption given by CEB-FIP. Overall, a water absorption value of less than 3% is classified as "good"- according to CEB-FIP's recommendations while CEB-FIP specifies concrete with typical absorption values in the range of 3 to 5% as "average" concrete [154]. From the results given in Tables 4.6 and 4.7, it can be seen that the absorption values of all the SCGC mix specimens are lower than 3%, the limit specified for good concretes. It has been reported that absorption values below 3% can be related to concretes with good durability. Based on this, it is possible to classify SCGC as concrete, which has the potential to be highly durable, in comparison to the OPC concrete. However, further studies relating to water, chloride and carbonate ingress into this type of concrete is necessary before such a conclusion may be definitively proclaimed.

Table 4.6 Water Absorption of SCGC Mix (Cubical Specimens)

Specimen No.	Actual Weight	Weight after oven drying (W_1)	Weight after 48 hrs of water soaking (W_2)	Water Absorption = $[(W_2-W_1)/W_1] \times 100$
	kg	kg	kg	%
1	2.284	2.232	2.295	2.82
2	2.335	2.278	2.341	2.77
3	2.392	2.341	2.405	2.73
Average				2.77

Table 4.7 Water Absorption of SCGC Mix (Cylindrical Specimens)

Specimen No.	Actual Weight	Weight after oven drying (W_1)	Weight after 48 hrs of water soaking (W_2)	Water Absorption = $[(W_2-W_1)/W_1] \times 100$
	kg	Kg	kg	%
1	3.611	3.516	3.619	2.93
2	3.637	3.539	3.641	2.88
3	3.653	3.559	3.664	2.95
Average				2.92

Table 4.8 Water Absorption of OPC Control Mix (Cubical Specimens)

Specimen No.	Actual Weight	Weight after oven drying (W_1)	Weight after 48 hrs of water soaking (W_2)	Water Absorption = $[(W_2-W_1)/W_1] \times 100$
	kg	kg	kg	%
1	2.376	2.318	2.420	4.40
2	2.353	2.301	2.399	4.26
3	2.415	2.367	2.469	4.31
Average				4.32

Table 4.9 Water Absorption of OPC Control Mix (Cylindrical Specimens)

Specimen No.	Actual Weight	Weight after oven drying (W_1)	Weight after 48 hrs of water soaking (W_2)	Water Absorption = $[(W_2-W_1)/W_1] \times 100$
	kg	kg	kg	%
1	3.729	3.665	3.828	4.45
2	3.692	3.633	3.797	4.51
3	3.658	3.593	3.756	4.54
Average				4.50

Table 4.10 Assessment Criteria for Absorption as per CEB-FIP [154]

Absorption (%)	Absorption rating	Concrete quality
< 3.0	low	good
3.0 to 5.0	average	average
> 5.0	high	poor

4.5.2 Mechanical Properties

4.5.2.1 Compressive Strength

The average compressive strength results of selected SCGC and OPC control mixtures up to 180 days are presented in Table 4.11 and Figure 4.23. Compressive strength was measured on 3rd, 7th, 28th, 90th and 180th day after casting of specimens. Unlike Portland cement concrete, geopolymer-based concretes are known to set rapidly and attain a significant percentage of their total compressive strength value within the first few hrs of reaction. This phenomenon became true in the present investigation. Although both SCGC and OPC had similar mix compositions with respect to the amount of binder and activator/binder ratio, however, as expected, SCGC mix specimens developed higher compressive strengths at earlier ages predominantly within the first 3 days, with little further development to later ages. It was found that SCGC mix specimens at 3rd day achieved over 90% of their 28-days compressive strength.

Compared to OPC concrete, heat-cured SCGC mix specimens produced higher compressive strengths at 3 and 7 days, but lower values at 90 and 180 days while at 28-days, SCGC mix developed almost similar strength to the control mixture. At early ages up to 7 days, fly ash-based SCGC exhibited about 30% higher strength while at later ages up to 180 days, SCGC mix gave about 14% lower values than the water-cured OPC concrete.

Test results indicated that the early age compressive strength of fly ash-based SCGC was much higher than that of OPC-based concrete. As the age of concrete progressed, the compressive strength increased both in SCGC and OPC mixes however, the rate of strength gain was more in OPC mix specimens than SCGC mix. As given in Table 4.11, after 3 days and 7 days, fly ash-based SCGC achieved about 91% and 96% of its 28 days compressive strength respectively whereas OPC-based control concrete gained about 55% and 73% of its 28 days compressive strength respectively. However, after 90 days and 180 days, SCGC developed only about 1.4% and 1.7% increment in strength respectively whereas OPC concrete exhibited about

11% and 17% increment in strength respectively as compared to the 28 days strength. This is because heat-cured geopolymer-based concretes considerably differ from OPC-based concretes in terms of matrix formation and strength gain, as geopolymer-based materials have a distinct setting and hardening behaviour and use very different reaction pathway in order to attain structural integrity. Unlike OPC concretes, which undergo a hydration process and form calcium-silicate-hydrates (CSH) for matrix formation and strength, geopolymer-based concretes involve a geopolymerization process to attain structural strength. The geopolymerization process, which is known to consist of the dissolution of source material species in the alkali medium, transferring of the dissolved species from the solid surface to gel phase, and condensation of the alumino-silicate gel phase, starts immediately as the alkali solution comes into contact with the source material. Consequently, the reaction product is generated and the silicate and aluminate species are formed. Continuous dissolution and reaction of the silicate and aluminate species result in the formation of an alkali alumino-silicate gel, which provides matrix formation and strength of geopolymer concrete [19, 47]. A schematic formation of a geopolymeric material can be seen in Figure 4.24. Because the chemical reaction of the heat-cured geopolymeric concrete is a fast polymerization process, initial reactivity is intense and occurs quickly upon activation, yet reaction products eventually coat remaining unreacted pozzolan particles and reduce the efficiency of activation. As the activator slowly permeates through the newly formed coating, the reaction continues at a slower rate, and the compressive strength continues to rise but does not vary greatly with the age of concrete [64]. This is in contrast to the strength development behaviour of OPC-based concretes, which gain strength with age.

Table 4.11 Compressive Strength of SCGC and OPC Mix Specimens at Various Ages

Age at Testing (Days)	Mean Compressive Strength (MPa)			
	SCGC Mix	Percent gain with reference to 28 days strength	OPC Control Mix	Percent gain with reference to 28 days strength
3	46.98	91.35	28.46	54.64
7	49.25	95.76	37.89	72.74
28	51.43	100	52.09	100
90	52.17	101.44	57.75	110.86
180	52.29	101.67	60.94	116.99

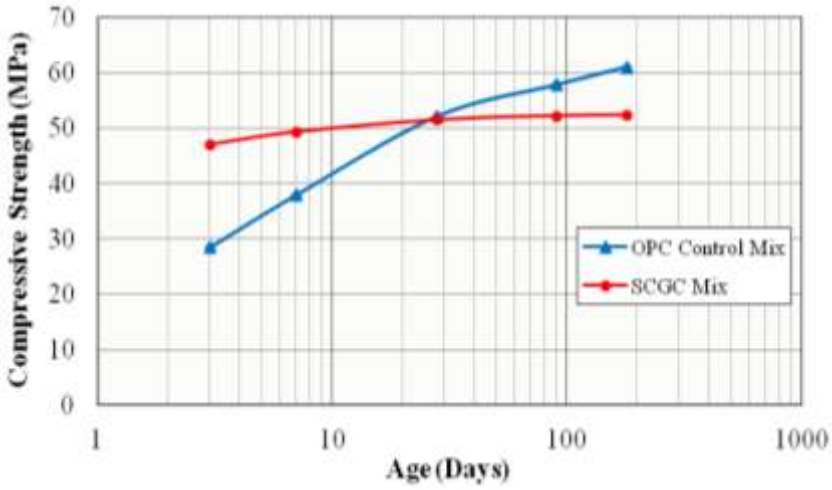

Figure 4.23 Strength Development of SCGC and OPC Mixes with Time

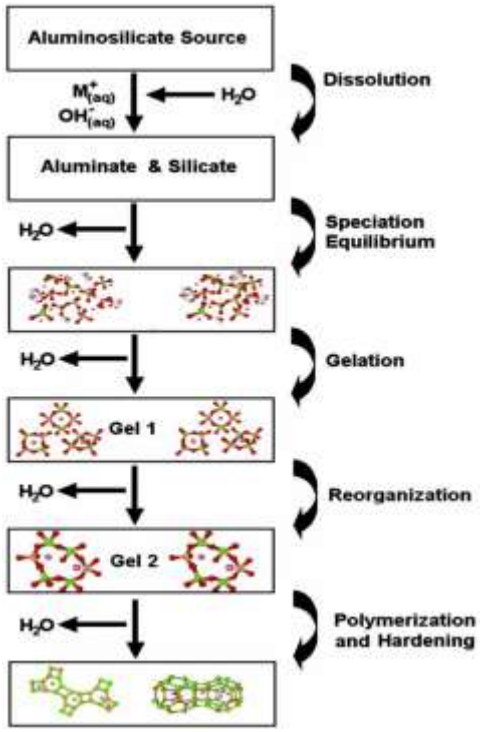

Figure 4.24 Conceptual Model for Geopolymerization [18]

4.5.2.2 Tensile Strength

The average splitting tensile strength results for both SCGC and OPC control mixtures at the age of 3, 7, 28 and 90 days after casting, are presented in Table 4.12 and Figure 4.25. For an easier comparison, the correlation between the compressive and the tensile strengths for these two types of concrete are also calculated. An

illustration of this comparison is presented in Table 4.13. From the test results, it can be seen that the trend in tensile strength is almost similar to that obtained for compressive strength. As in the case of compressive strength test, SCGC mix specimens developed very high tensile strengths at early ages, and exhibited lower values at 28 days and 90 days than the corresponding OPC mix specimens. Similarly, at later ages, the rate of strength gain was more in OPC mix than SCGC mix. At early ages up to 7 days, fly ash-based SCGC exhibited about 22% higher tensile strength while at later ages up to 90 days, SCGC mix produced about 6% lower values than the OPC-based concrete. After 3 days and 7 days, fly ash-based SCGC achieved about 93% and 98 % of its 28 days tensile strength respectively whereas OPC-based control concrete gained about 66% and 80% of its 28 days value respectively. However, after 90 days, SCGC developed only about 0.5% increment in strength whereas OPC concrete exhibited about 5.5% increment in strength as compared to the 28 days strength.

The results given in Table 4.13 indicate that the splitting tensile strength of SCGC is only a fraction of its compressive strength, as in the case of Portland cement concrete. Tensile strength values of SCGC are between 7.97 to 8.26% of compressive strength. On average, the splitting tensile strength of SCGC is about 8.11% of its compressive strength, which is in good agreement with the range reported for normal strength Portland cement concrete. Sofi et al. [61] also performed indirect tensile strength tests on geopolymer mortar and concrete specimens. The trend of test results observed in that study is similar to that observed in the results given in Table 4.13.

Table 4.12 Splitting Tensile Strength of SCGC and OPC Mix Specimens at Different Ages

Age at Testing (Days)	Mean Slitting Tensile Strength (MPa)			
	SCGC Mix	Percent gain with reference to 28 days strength	OPC Control Mix	Percent gain with reference to 28 days strength
3	3.84	92.75	2.77	66.11
7	4.07	98.31	3.34	79.71
28	4.14	100	4.19	100
90	4.16	100.48	4.42	105.49

Table 4.13 Correlation between Compressive Strength and Tensile Strength of SCGC and OPC Mix

Mix ID	Age at Testing (Days)	Mean Compressive Strength (MPa)	Mean Splitting Tensile Strength (MPa)	Tensile Strength as a % Value of Compressive Strength	Average
SCGC	3	46.98	3.84	8.17%	8.11%
	7	49.25	4.07	8.26%	
	28	51.43	4.14	8.05%	
	90	52.17	4.16	7.97%	
OPC Control Mix	3	28.46	2.77	9.73%	8.56%
	7	37.89	3.34	8.81%	
	28	52.09	4.19	8.04%	
	90	57.75	4.42	7.65%	

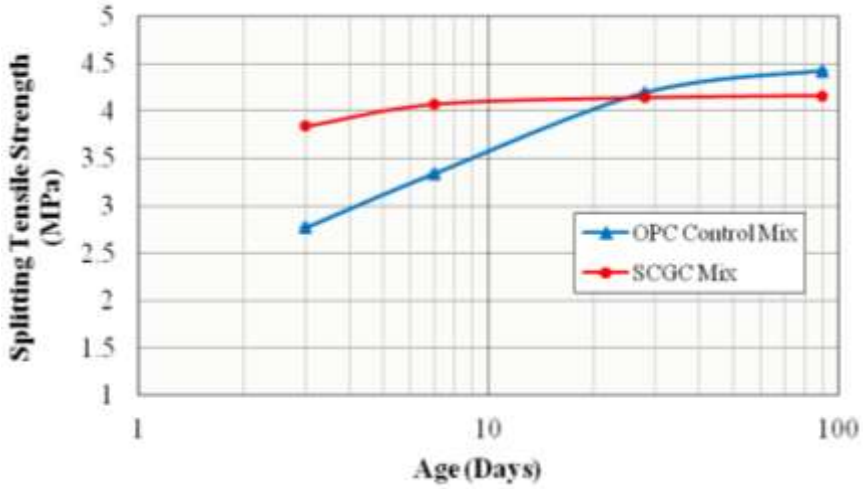

Figure 4.25 Splitting Tensile Strength of SCGC and OPC Mixes at Various Ages

Experimentally determined values of splitting tensile strength of SCGC were also compared with the analytical models given by Neville [37], ACI Building Code 318 [155], ACI Committee 363 [156], Eurocode 2 [157], Felekoglu et al. [107] and Parra et al. [76] (Equations 4.1-4.6 respectively) and results are given in Table 4.14 and shown in Figure 4.26.

$$fct = 0.3\ \{f'_c\}^{2/3} \quad (4.1)$$

$$fct = 0.56\ \sqrt{f'_c} \quad (4.2)$$

$$fct = 0.59\ \sqrt{f'_c} \quad (4.3)$$

$$fct = 2.35\ ln(1 + f'_c/10) \quad (4.4)$$

$$fct = 0.43\ (f'_c)^{0.6} \quad (4.5)$$

$$fct = 0.28\ \{(f'_c)^{2/3} \quad (4.6)$$

where, *fct* = Splitting Tensile strength (MPa) and
f'_c = Compressive strength (MPa)

The calculated values of splitting tensile strength using Equations 4.1-4.6 show that the measured indirect tensile strength of fly ash-based SCGC falls within the range and compares favourably with the models presented by the different standards for Portland cement concrete. The constant of proportionality, calculated as square root of their compressive strengths, was in the range of 0.56 to 0.58 which is reasonably close to the values of 0.56 and 0.59, suggested by ACI 318 [155] and ACI 363 [156] respectively. Figure 4.26 depicts that the relationship between compressive and splitting tensile strength obtained experimentally is slightly above or equal to the majority of code provisions. This shows that for the same compressive strength, the splitting tensile strength of SCGC satisfies the design equations given by different standards and codes for Portland cement concrete.

Table 4.14 Comparison between Calculated Values using Equations 4.1-4.6 and Measured Splitting Tensile Strength of SCGC

Age at Testing (Days)	Measured Tensile Strength (MPa)	Splitting Tensile Strength (MPa) by					
		Neville [37] Equation 4.1	ACI 318 [155] Equation 4.2	ACI 363 [156] Equation 4.3	Eurocode 2 [157] Equation 4.4	Felekoglu et al.[107] Equation 4.5	Parra et al.[76] Equation 4.6
3	3.84	3.90	3.84	4.04	4.09	4.33	3.64
7	4.07	4.03	3.93	4.14	4.18	4.45	3.76
28	4.14	4.15	4.02	4.23	4.26	4.57	3.87
90	4.16	4.19	4.04	4.26	4.29	4.61	3.91

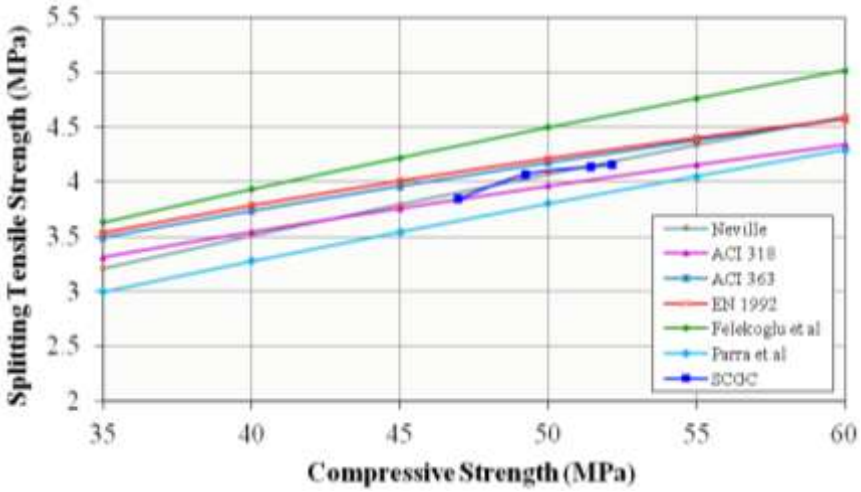

Figure 4.26 Comparison of Experimentally Determined Tensile Strength Values of SCGC with Analytical Models

4.5.2.3 Flexural Strength

Flexural strength test results of SCGC and reference OPC mix specimens at the age of 3, 7, 28 and 90 days after casting are shown in Table 4.15 and Figure 4.27. The coefficient of modulus of rupture (MOR) is also calculated for both mixes and the results are presented in Table 4.16. From the test results, it can be seen that similar to compressive and tensile strengths, the flexural strength values of SCGC are higher at earlier ages and lower at longer ages than the values of OPC control concrete. As the age of concrete increased the flexural strength increased both in SCGC and OPC mixes but the rate of increase was more in OPC mix than SCGC mix. As shown in Table 4.15, at early ages up to 7 days, fly ash-based SCGC exhibited about 5% higher flexural strength while at later ages up to 90 days, SCGC mix produced about 11% lower values than the OPC-based concrete. After 3 days and 7 days, fly ash-based SCGC achieved about 89% and 92% of its 28 days flexural strength respectively whereas OPC-based control concrete achieved about 67% and 80% of its 28 days value respectively. However, after 90 days, SCGC developed only about 0.24% increment in strength whereas OPC concrete exhibited about 3% increment in strength as compared to the 28 days strength.

Test results indicate that the flexural strengths of SCGC and OPC concrete do not necessarily follow the trend of their compressive strengths. Even when the

compressive strengths of both concrete types were approximately equal, the flexural strength of OPC concrete was slightly higher than that of SCGC. Compared to values between 7.95% and 10.47% of compressive strength, exhibited by OPC mix specimens, flexural strength values of SCGC mix remained between 7.63% and 7.95% of their compressive strength. On average, the flexural strength of SCGC was about 8% of its compressive strength, which is slightly lower than the range of 10-20% assigned for OPC-based concretes. The exact reason for this behavior though unclear, yet this may be due to the different type of curing which affected the flexural strength of SCGC and resulted lower values. Reduced flexural strength of heat-cured SCGC mix specimens can also be attributed to the presence of drying shrinkage strains observed on the surfaces of the specimens, causing premature failure and forcing the beam specimens to break at a lower load resulting in reduced flexural strength values.

Table 4.15 Flexural Strength of SCGC and OPC Mix Specimens at Different Ages

Age at Testing (Days)	Mean Flexural Strength (MPa)			
	SCGC Mix	Percent gain with reference to 28 days strength	OPC Control Mix	Percent gain with reference to 28 days strength
3	3.62	88.51	2.98	66.82
7	3.76	91.93	3.57	80.04
28	4.09	100	4.46	100
90	4.10	100.24	4.59	102.91

Table 4.16 Co-efficient of MOR for SCGC and OPC Mix

Mix ID	Age at Testing (Days)	Mean Compressive Strength (MPa)	Mean Flexural Strength (MPa)	Co-efficient of MOR $\alpha = f_r / \sqrt{f'_c}$	Flexural strength as a % Value of Compressive strength	Average
SCGC	3	46.98	3.62	0.528	7.71%	7.79%
	7	49.25	3.76	0.536	7.63%	
	28	51.43	4.09	0.570	7.95%	
	90	52.17	4.10	0.568	7.86%	
OPC Control Mix	3	28.46	2.98	0.558	10.47%	9.10%
	7	37.89	3.57	0.580	9.42%	
	28	52.09	4.46	0.618	8.56%	
	90	57.75	4.59	0.604	7.95%	

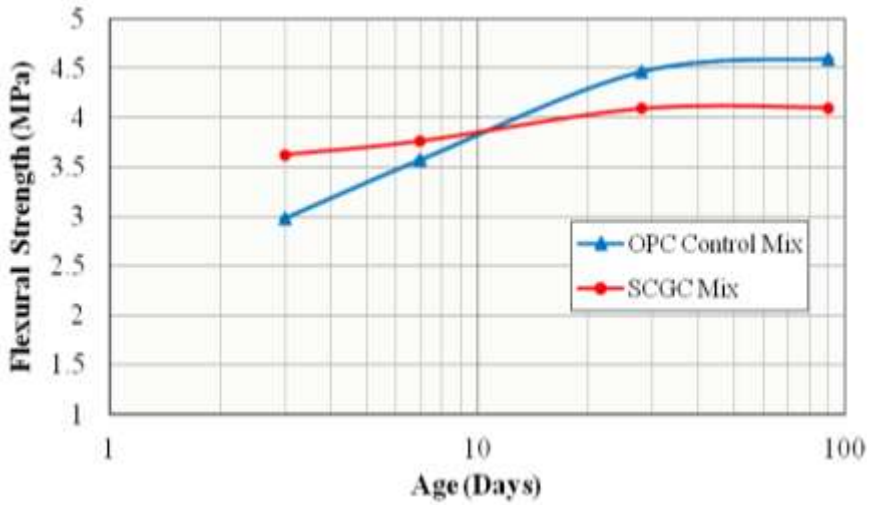

Figure 4.27 Flexural Strength of SCGC and OPC Mixes at Various Ages

To corroborate the results, like splitting tensile strength, experimentally determined values of flexural strength of SCGC were also compared with the available models suggested by ACI 318 [155] and ACI 363 [156] (Equations 4.7 and 4.8, respectively) and results are presented in Table 4.17 and Figure 4.28.

$$f_r = 0.62 \sqrt{f'_c} \quad (4.7)$$

$$f_r = 0.94 \sqrt{f'_c} \quad (4.8)$$

where, f_r = Flexural sterngth (MPa) and
f'_c = Compressive strength (MPa)

From the results shown in Table 4.17 and Figure 4.28, it can be seen that flexural strength values of SCGC mix at all testing ages are lower than those calculated by the ACI 318 [155] and ACI 363 [156] equations. The coefficient for MOR, calculated as square root of their compressive strengths, found to be in the range of 0.53 to 0.57, which is lower than those of 0.62 and 0.94, suggested by ACI 318 [155] and ACI 363 [156] respectively. Figure 4.28 exemplifies that the relationship between compressive and flexural strength obtained experimentally is below to the considered formulations, which shows that these models considerably overestimate the flexural strength of SCGC. Therefore, future investigations are required in order to devise appropriate formulations to predict flexural strength of SCGC.

Table 4.17 Comparison between Calculated Values using Equations 4.7 and 4.8 and Measured Flexural Strength of SCGC

Age at Testing (Days)	Measured Compressive Strength (MPa)	Measured Flexural Strength (MPa)	Flexural Strength (MPa) by	
			ACI 318 [155] Equation 4.7	ACI 363 [156] Equation 4.8
3	46.98	3.62	4.25	6.44
7	49.25	3.76	4.35	6.59
28	51.43	4.09	4.45	6.74
90	52.17	4.10	4.48	6.79

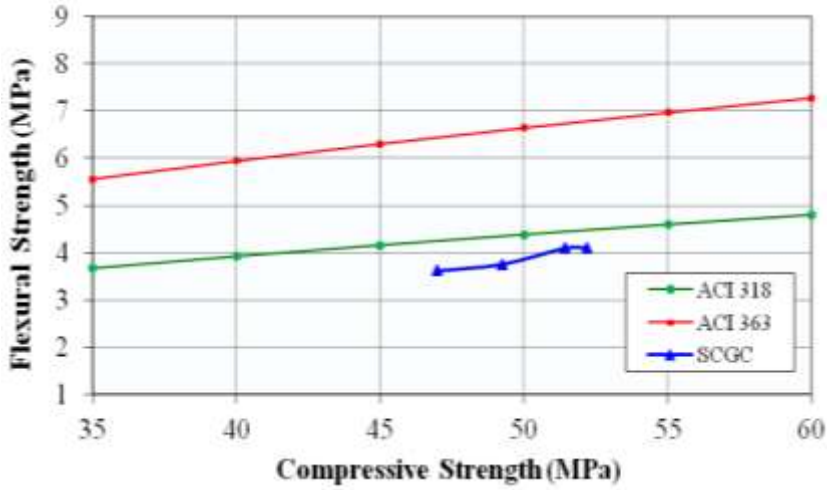

Figure 4.28 Comparison of Experimentally Determined Flexural Strength Values of SCGC with Analytical Models

4.6 Use of Silica fume as a Partial Replacement of Fly ash in SCGC

Silica fume, one of the most popular pozzolanas, is used in Portland cement concrete to get improved properties. In the present study, due to lower values of tensile and flexural strengths of SCGC, it was decided to use silica fume as a partial replacement of fly ash. For this purpose, four mixtures, one control mix without silica fume and three other mixes with different proportions of silica fume, were prepared. Fly ash was replaced with silica fume at the contents of 5%, 10%, and 15% by mass. All the other mix parameters were kept constant. The mixture designation and the quantities of various materials for each designed concrete mix are given in Table 4.18.

Table 4.18 Mix Proportions

Materials	$SCGCM_1$ (0% SF)	$SCGCM_2$ (5% SF)	$SCGCM_3$ (10% SF)	$SCGCM_4$ (15% SF)
Fly Ash (kg/m^3)	400	380	360	340
Silica Fume (kg/m^3)	0	20	40	60
Fine Aggregate (kg/m^3)	850	850	850	850
Coarse Aggregate (kg/m^3)	950	950	950	950
Sodium Hydroxide (kg/m^3)	57	57	57	57
Concentration (M)	10	10	10	10
Sodium Silicate (kg/m^3)	143	143	143	143
Superplasticizer (%)	6	6	6	6
Extra water (%)	12	12	12	12
Curing Time (hrs)	48	48	48	48
Curing Temperature (°C)	70	70	70	70

4.6.1 Analysis of Results

4.6.1.1 Fresh Properties

The results of fresh properties of various SCGC mixes with the different contents of silica fume are presented in Table 4.19. Fresh properties were assessed using Slump flow, V-Funnel and L-Box test methods following the European guidelines (EFNARC) for SCC [11, 92]. As reported in literature, because of the higher surface area and extremely fine particle size, silica fume increases the water requirement of concrete, consequently, reduces the workability of fresh concrete. This hypothesis became true in this investigation. The addition of silica fume as a partial replacement of fly ash in SCGC resulted in the loss of workability. This might be explained by the increased surface area of silica fume particles. Generally, the mixtures containing silica fume exhibited worse performance than the control mixture in regards to the fresh properties. Silica fume, because of its higher surface area than fly ash, absorbed the excessive water in geopolymer system. It was observed that the concrete mixes containing higher percentages of silica fume were more cohesive and appeared to be sticky; and the fluidity and flowability of various SCGC mixtures were reduced when

the proportion of silica fume increased. These effects of silica fume on fresh properties of SCGC were consistent with the results reported by Andri [158], who found that the workability of freshly prepared fly ash-based geopolymer concrete was decreased with the increase in the quantity of silica fume. SCGC mixes had a slump flow in the range of 640-695 mm, flow time in the range of 3.5-6.5 sec, V-Funnel time in the range of 9-15 sec and L-Box ratios were greater than 0.8 for all mixes. Although the fluidity and flowability of various SCGC mixes decreased when the content of silica fume increased, nevertheless, concrete mixes still met the requirements of flowability, viscosity, and passing ability of SCC with the silica fume addition up to 10% by mass of fly ash. Based on the assessment of fresh properties of SCGC, it can be concluded that silica fume can be used in the production of SCGC up to 10% by mass of fly ash.

Table 4.19 Fresh Properties of various SCGC Mixes with the different contents of Silica fume

Mix ID	Slump flow		V-Funnel flow time (sec)	L-Box blocking ratio (H_2/H_1)
	Diameter (mm)	$T_{50\ cm}$ (sec)		
EFNARC range [92]	650-800	2-5	6-12	0.8-1
$SCGCM_1$ (0% SF)	695	3.5	9	0.96
$SCGCM_2$ (5% SF)	680	4.0	9.5	0.96
$SCGCM_3$ (10% SF)	665	4.5	11	0.94
$SCGCM_4$ (15% SF)	640	6.5	15	0.90

4.6.1.2 Hardened Properties

In the hardened state, compressive, splitting tensile and flexural strengths were investigated. All of these tests were performed at the ages of 3, 7 and 28 days after casting. The results of these tests are discussed in the following sub-sections.

4.6.1.2.1 Compressive Strength

Table 4.20 and Figure 4.29 illustrate the compressive strength test results of various SCGC mixes with and without silica fume. In order to assess the effect of silica fume

addition in terms of silica content in the mix on the compressive strength of SCGC, the molar ratios SiO_2/Al_2O_3 and SiO_2/Na_2O were also calculated. The calculation for these molar ratios is given in Appendix A. The inclusion of silica fume as a partial replacement of fly ash in SCGC was found to be effective in improving the hardened properties of concrete. From Table 4.20, it can be seen that the compressive strength of fly ash-based SCGC with 5%, 10%, and 15% silica fume replacement are higher than the Mix $SCGCM_1$ (0% SF) at every age of testing. At 28 days, the Mixture $SCGCM_1$ (0% SF) achieves a compressive strength of 51.43 MPa, whereas mixtures $SCGCM_2$ (5% SF), $SCGCM_3$ (10% SF), and $SCGCM_4$ (15% SF) achieve a compressive strength of 53.38, 55.02, and 53.96 MPa, respectively, an increase of 3.8%, 7.0%, and 4.9% in comparison with the strength of control mixture. Test results indicate that, until the 10% of silica fume, the higher the percentage of silica fume, the higher the values of compressive strength; after that, the increase in the percentage of silica fume leads to the decrease in compressive strength.

The increase in compressive strength with the inclusion of silica fume was due to the fact that the silica fume is finer than fly ash, which resulted in the dense particle packing, pore size refinement, and denser concrete matrix. When the fine silica fume was added in the SCGC mixes, it offered the active SiO_2, which is advantageous to form the siloxo bridges (–Si–O–Si–O–) during the geopolymerization processing. These bridge chains bond the particles firmly, and a much denser and more compact matrix structure is formed; consequently, both compressive and bending strengths are enhanced [159]. In addition, due to higher silica content, the SiO_2/Al_2O_3 molar ratio was increased in the mixtures (Table 4.20). The SiO_2/Al_2O_3 molar ratio is an extremely important parameter, which has major influence on the physical and mechanical characteristics as well as on its microstructure. The mechanical strength of the geopolymeric materials is known to be increased by a higher SiO_2/Al_2O_3 ratio, as with increasing SiO_2/Al_2O_3 ratio, polysialatesiloxo and polysialatedisiloxo structures become dominant, which have more strength and stiffness in comparison to polysialate structures [45, 52]. Also, more Si–O–Si bonds are formed in the final product, which are stronger in comparison to Si–O–Al and Al–O–Al bonds, resulting in higher mechanical strength [160]. Moreover, the additional dissolution and polycondensation processes of aluminate precursors from the fly ash particles with

silicate monomer and oligomer supplied by silica fume particles results in an improved geopolymer matrix with denser gel structure, which lead to the higher bending and compressive strengths [158].

However, experimental results indicate that the compressive strength of SCGC decreased when the addition of silica fume passed over 10% by mass of fly ash (SiO_2/Al_2O_3 ratio increased from 4.10 to 4.46). The silica content (SiO_2/Al_2O_3 ratio) controls the dissolution and polymerization of Si and Al in aluminosilicate gel. With increasing SiO_2/Al_2O_3 ratio, the solubility and gel formation decreases [144]. Increasing the silica fume content beyond 10% resulted in a negative effect by forming agglomerates, which hindered geopolymerization reactions and inhibited the propagation of three-dimensional geopolymer networks [41]. Too high silica (SiO_2/Al_2O_3) content caused by the continuous increase of silica fume in the geopolymer mix leads to the formation of a two-dimensional cross-linked poly-sialate that is known to lower the mechanical properties as compared with a three-dimensional geopolymer network [41]. Furthermore, continuous increase in silica (SiO_2/Al_2O_3) content led to insufficient wetting of the medium that hinder the propagation of geopolymer chains and so weaken its mechanical properties [41]. This is because, with the increasing addition of silica fume in the geopolymer mix, if the alkali concentration remains same (as in the present case where sodium hydroxide content was kept constant for all the four mixtures) the reactive silica becomes unreactive due to insufficient concentration of hydroxyl ions resulting incomplete geopolymerization and consequently leading to lower mechanical properties.

Table 4.20 Compressive Strength Test Results

Mix ID	Molar Ratio		Compressive strength (MPa)					
	SiO_2/Al_2O_3	SiO_2/Na_2O	3-Days	Percent Increase	7-Days	Percent Increase	28-Days	Percent Increase
$SCGCM_1$ (0% SF)	3.48	6.77	46.98	-	49.25	-	51.43	-
$SCGCM_2$ (5% SF)	3.78	7.00	48.22	2.6	51.62	4.8	53.38	3.8
$SCGCM_3$ (10% SF)	4.10	7.22	50.25	7.0	53.76	9.2	55.02	7.0
$SCGCM_4$ (15% SF)	4.46	7.45	48.84	4.0	51.55	4.7	53.96	4.9

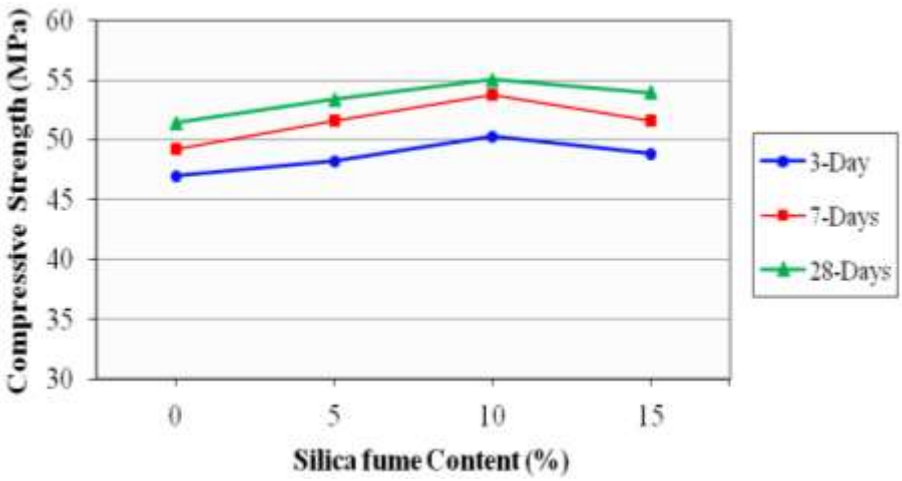

Figure 4.29 Effect of Silica fume on Compressive Strength

4.6.1.2.2 Splitting Tensile Strength

The relationships between tensile, flexural, and compressive strengths in fly ash-based SCGC containing silica fume were found to be almost similar as in case of OPC concrete. An increase in the compressive strength generally resulted in a similar relative increase in the tensile and flexural strengths. The splitting tensile strength test results of various SCGC mixes with and without silica fume are given in Table 4.21 and Figure 4.30. From Figure 4.30, it can be seen that, there is an increase in splitting tensile strength with the increase in silica fume contents; however, the maximum strength at all ages occurs at 10% fly ash replacement. With increasing the amount of silica fume content over 10%, splitting tensile strength decreases. The same reasons and mechanism mentioned for compressive strength are commanding the explanations for the results of split tensile strength test. The results indicate that the trend in the splitting tensile strength with silica fume content is almost similar to that in the case of compressive strength. At 28 day, the splitting tensile strength of $SCGCM_1$ (0% SF) achieves 4.14 MPa, whereas mixtures $SCGCM_2$ (5% SF), $SCGCM_3$ (10% SF), and $SCGCM_4$ (15% SF) achieve strengths of 4.31, 4.67, and 4.24 MPa, respectively, an increase of 4.1%, 12.8%, and 2.4% in comparison with the strength of control mix.

Table 4.21 Splitting Tensile Strength Test Results

Mix ID	Splitting tensile strength (MPa)					
	3-Days	Percent Increase	7-Days	Percent Increase	28-Days	Percent Increase
$SCGCM_1$ (0% SF)	3.84	-	4.07	-	4.14	-
$SCGCM_2$ (5% SF)	3.92	2.1	4.18	2.7	4.31	4.1
$SCGCM_3$ (10% SF)	4.12	7.3	4.40	8.1	4.67	12.8
$SCGCM_4$ (15% SF)	3.89	1.3	4.09	0.5	4.24	2.4

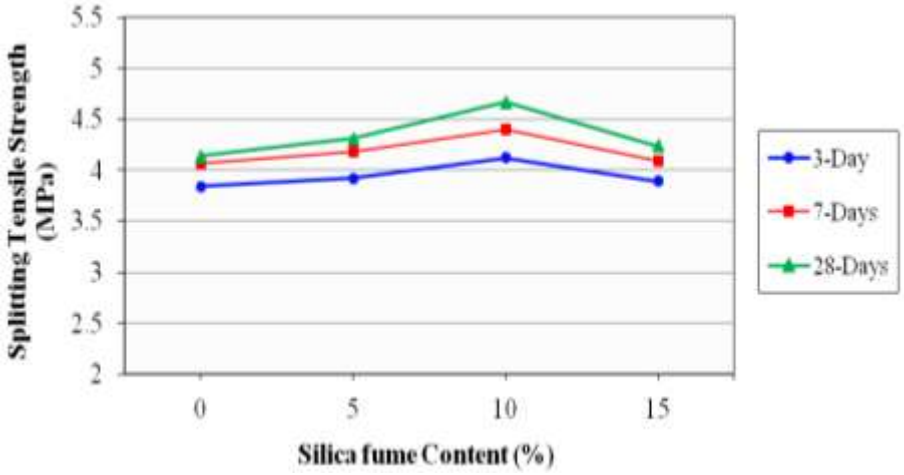

Figure 4.30 Effect of Silica fume on Splitting Tensile Strength

4.6.1.2.3 Flexural Strength

The flexural strength test results for SCGC mixes with different contents of silica fume are given in Table 4.22 and Figure 4.31. Like compressive and splitting tensile strengths, silica fume addition also improved the flexural strength of SCGC mixes; however, its inclusion appeared to have a more pronounced effect on the flexural strength than the compressive and split tensile strengths. This might be due to the improved interfacial bond between the paste and aggregates. The flexural strengths of SCGC almost followed the same trend as the compressive strength and tensile strength did. From Figure 4.31, it can be seen that the flexural strength of SCGC increases with the increase in silica fume content up to 10% replacement of fly ash and then tends to decrease. At 28 day, the flexural strength of $SCGCM_1$ (0% SF) achieves 4.09 MPa, whereas mixtures $SCGCM_2$ (5% SF), $SCGCM_3$ (10% SF), and

$SCGCM_4$ (15% SF) achieve strengths of 4.18, 4.56, and 4.21 MPa, respectively, an increase of 2.2%, 11.5%, and 2.9% in comparison with the strength of control mix.

Table 4.22 Flexural Strength Test Results

Mix ID	Flexural strength (MPa)					
	3-Days	Percent Increase	7-Days	Percent Increase	28-Days	Percent Increase
$SCGCM_1$ (0% SF)	3.62	-	3.76	-	4.09	-
$SCGCM_2$ (5% SF)	3.80	5.0	4.03	7.2	4.18	2.2
$SCGCM_3$ (10% SF)	3.98	9.9	4.29	14.1	4.56	11.5
$SCGCM_4$ (15% SF)	3.78	4.4	4.10	9.0	4.21	2.9

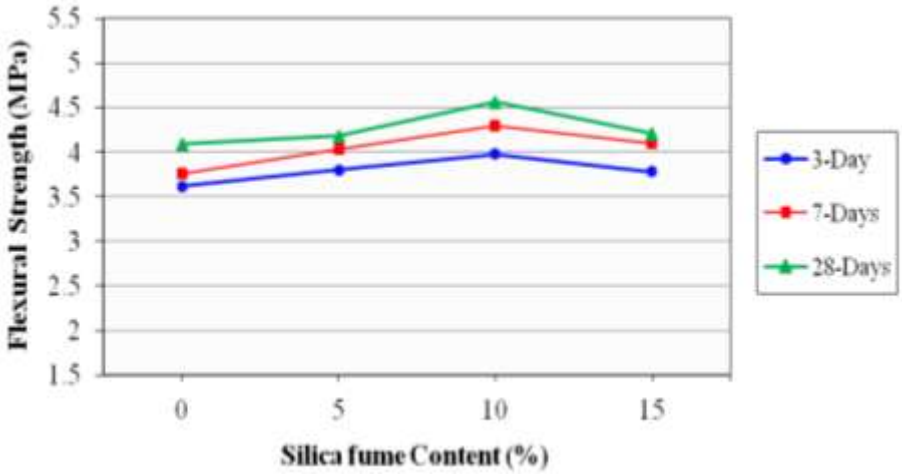

Figure 4.31 Effect of Silica fume on Flexural Strength

4.7 Modulus of Elasticity

For determining the values for modulus of elasticity and Poisson's ratio, two SCGC and one OPC-based control mixture (Table 3.10) were manufactured. The static modulus of elasticity was determined on 100 x 200 mm cylindrical specimens in accordance with ASTM C 469 [139]. At the end of appropriate curing regime, duplicate set of specimens from each mix were tested at the ages of 3, 7 and 28 days. The average values of modulus of elasticity obtained from two individual specimens for each concrete mix at different ages are presented in Table 4.23 and Figure 4.32. The calculations for modulus of elasticity are given in Appendix D.

From the test results, it can be seen that the modulus of elasticity increases with increasing compressive strength. The early age modulus of elasticity is important in the precast/prestressed industry for investigating effects such as elastic shortening. Test results indicate that at 3-day the modulus of elasticity of heat-cured SCGC specimens is about 90 % of its 28-day value.

The use of supplementary cementitious materials in concrete is reported to have generally no effect or slight increase in the modulus of elasticity of Portland cement concrete [39]. In the present study, the use of silica fume was also found to have marginal effect on the elastic modulus of SCGC. Test results show that replacement of fly ash with 10% silica fume slightly increased the modulus of elasticity of concrete. At 28-day, SCGC specimens with 10% silica fume, achieved a modulus of elasticity of 22.341 GPa in comparison to the value of 21.402 GPa, exhibited by 100% fly ash-based SCGC specimens, an increase of 4.4%.

In contrast to the higher strength of SCGC compared to that of OPC control concrete, it can be seen that the elastic moduli of both SCGC mixes are lower than those of OPC control mix. The static modulus of elasticity of SCGC-1 and SCGC-2 mixes after 28 days were 21.40 and 22.34 GPa, respectively compared to OPC control mix, which displayed 28.26 GPa. These values are around 20% to 25% lower than associated OPC mix. It is believed that similar to OPC concrete, the elastic modulus of SCGC was influenced by the elastic modulus of the geopolymer paste and the elastic modulus of the aggregate. As, the same proportion of aggregates was used in all three mix specimens, variations in the elastic modulus of the aggregates can be considered to have a negligible effect on the elastic modulus of the resulting SCGC. Therefore, variations in the elastic modulus of SCGC can be contributed mainly to variations in the elastic modulus of the geopolymer paste [161].

As mentioned earlier, the static modulus of elasticity of SCGC measured in this study is about 20 to 25% lower than that of reference OPC concrete, which agrees with some of the results of other researchers. Olivia and Nikraz [48] in their study on fly ash-based geopolymer concrete found 15 to 30% lower values of elastic modulus than that of OPC-based concrete. Fernandez-Jimenez et al. [69] also found much lower modulus of elasticity for fly ash-based geopolymer concrete, who revealed that

alkali activated fly ash based concrete showed a much lower static modulus of elasticity than expected. The values presented for normal Portland cement concrete ranged from 30.3 to 32.3 GPa while for geopolymeric concrete they ranged from 10.7 to 18.4 GPa. Hardjito and Rangan [1] however observed better elastic modulus values for fly ash-based geopolymer concrete. Using granite-type coarse aggregate, authors reported modulus of elasticity values of 23.0 GPa to 30.8 GPa for compressive strengths values ranging from 44 MPa to 89 MPa.

Table 4.23 Modulus of Elasticity of SCGC and OPC Mix Concretes at Different Ages

Mix ID	Age at Testing (Days)	Mean Compressive Strength (MPa)	Modulus of Elasticity (GPa)
SCGC-1	3	38.49	19.239
	7	40.18	20.013
	28	43.06	21.402
SCGC-2	3	40.47	19.736
	7	43.20	21.109
	28	46.55	22.341
OPC Control Mix	3	23.44	17.295
	7	31.90	23.714
	28	41.02	28.257

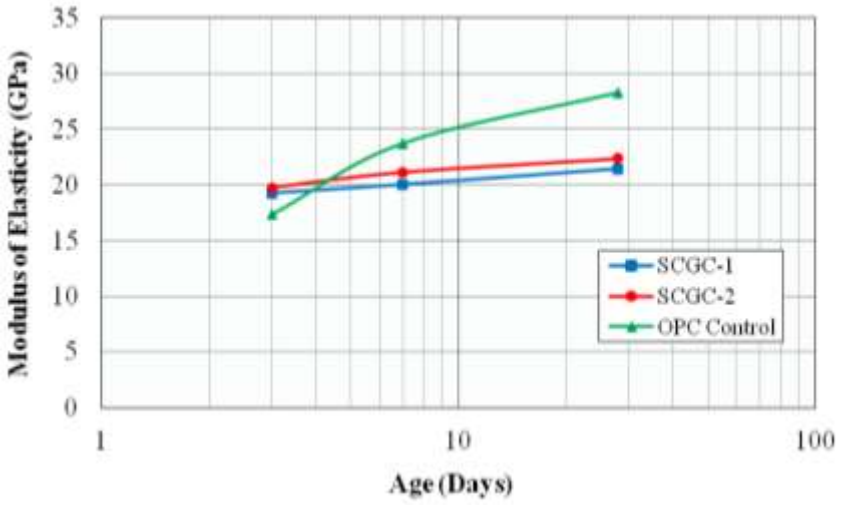

Figure 4.32 Modulus of Elasticity of SCGC and OPC Control Mixes at Various Ages

Comparison with Formulations

Applicability of available criterions to SCGC was also assessed by comparing available expressions for predicting elastic properties. Experimentally determined values of modulus of elasticity of both SCGC mixes were compared with the available models given by ACI 318 [155], ACI 363 [156] and Eurocode 2 [157] (Equations 4.9-4.11 respectively). In addition, specifically devised expressions for SCC by Persson [114] and Dinkar et al. [162] (Equations 4.12-4.13 respectively) were also compared. The modulus of elasticity of each mix determined by testing and the comparative values calculated by different equations are presented in Table 4.24 and Figure 4.33. For an easier comparison, the test/predicted ratios of the static elastic modulus based on the experimental results and the predicted values calculated by different equations are also included. An illustration of this comparison is given in Table 4.25.

$$E_c = 4730 \sqrt{f'_c} \quad (4.9)$$

$$E_c = 3320 \sqrt{f'_c} + 6900 \quad (4.10)$$

$$E_c = 21500 (f'_c /10)^{1/3} \quad (4.11)$$

$$E_c = 3750 \sqrt{f'_c} \quad (4.12)$$

$$E_c = 4180 \sqrt{f'_c} \quad (4.13)$$

where, E_c = static modulus of elasticity (MPa) and

f'_c = compressive strength (MPa)

From Table 4.24, it can be seen that the modulus of elasticity values for both SCGC mixes at all ages are lower than those predicted by considered models. The modulus of elasticity of SCGC determined from the experimental testing is about 60 to 90% of that predicted by theoretical equations. Figure 4.33 show that the relationship between compressive strength and modulus of elasticity obtained experimentally is below to the majority of the considered formulations. In comparing the measured modulus of elasticity values relative to the predicted values, for a given strength, all selected models overestimate this property of SCGC by far; except for

Persson [114] model which seems to give better estimation. This might be due to the lower coarse aggregate content in the SCGC mixes and the type of curing which affected the elastic modulus of SCGC. It is known that the modulus of elasticity of concrete depends on the proportion of the elastic modulus of the individual components and their percentages by volume. It increases for high contents of aggregates of high rigidity. A relatively small modulus of elasticity can be anticipated because of the low content of coarse aggregates [83]. Besides, all SCGC mix specimens for modulus of elasticity were tested in a dry condition. The ASTM C 469 [139] specifies that cylinders be tested in a moist condition. Testing specimens in a dry condition is known to reduce the modulus of elasticity, which could also be partially responsible for most of the elastic modulus measurements being lower than predicted by relevant standards.

Table 4.24 Comparison between Calculated Values using Equations 4.9-4.13 and Measured Values of Modulus of Elasticity

Mix ID	Age (days)	Experimental Modulus of Elasticity (GPa)	Modulus of Elasticity (GPa) by				
			ACI 318 [155] Equation 4.9	ACI 363 [156] Equation 4.10	Eurocode 2 [157] Equation 4.11	Persson [114] Equation 4.12	Dinkar et al. [162] Equation 4.13
SCGC-1	3	19.239	29.345	27.497	33.694	23.265	25.933
	7	20.013	29.982	27.945	34.180	23.770	26.496
	28	21.402	31.038	28.686	34.978	24.607	27.429
SCGC-2	3	19.736	30.090	28.020	34.262	23.856	26.591
	7	21.109	31.088	28.721	35.016	24.647	27.474
	28	22.341	32.272	29.551	35.899	25.585	28.519

Table 4.25 Test-to-Predicted Static Elastic Modulus Ratios

Mix ID	Age (days)	ACI 318	ACI 363	Eurocode 2	Persson	Dinkar et al.
SCGC-1	3	0.65	0.70	0.57	0.83	0.74
	7	0.67	0.72	0.58	0.84	0.75
	28	0.69	0.75	0.61	0.87	0.78
SCGC-2	3	0.65	0.70	0.58	0.83	0.74
	7	0.68	0.73	0.60	0.86	0.77
	28	0.69	0.76	0.62	0.87	0.78

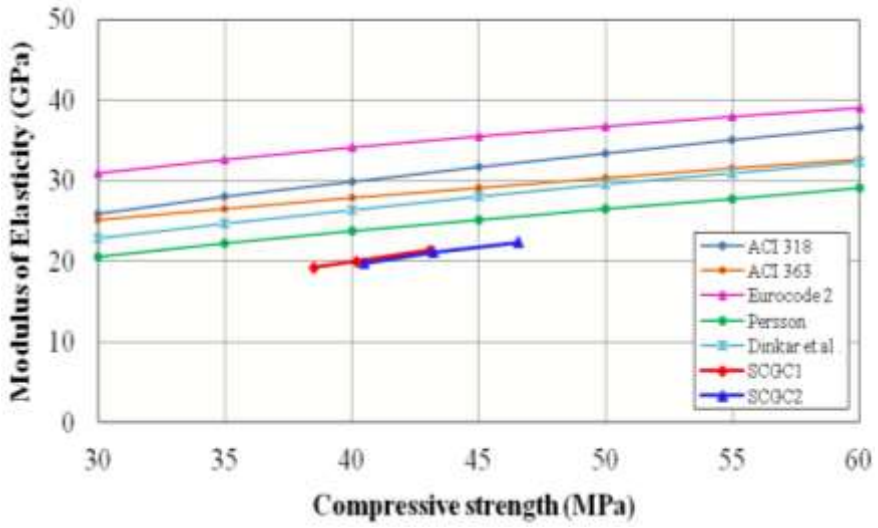

Figure 4.33 Comparison of Experimentally Determined Elastic Modulus of SCGC with Analytical Models

4.8 Poisson's Ratio

The values of Poisson's ratio for all mix compositions were measured and calculated, following the procedure outlined in ASTM C 469 [139]. The data required for Poisson's ratio was obtained simultaneously while collecting the data for modulus of elasticity. Table 4.26 presents the average values of Poisson's ratio for each mix investigated. The experimental values obtained for Poisson's ratio show an overall increase with the increase of compressive strength. It can be seen from Table 4.26 that the values of Poisson's ratio for all of the SCGC samples fall between 0.109 and 0.155, which are close to the range assigned for normal strength Portland cement concrete. For normal strength Portland cement concrete the value of Poisson's ratio lies generally in the range of 0.15 to 0.22 [37]. Hardjito and Rangan [1] used low-calcium fly ash to manufacture geopolymer concrete specimens. The measured values of Poisson's ratio reported in that study are in line with the results given in Table 4.26.

Table 4.26 Poisson's Ratio of SCGC and OPC Mixes at Different Ages

Mix ID	Age at Testing (days)	Mean Compressive Strength (MPa)	Poisson's Ratio
SCGC-1	3	38.49	0.114
	7	40.18	0.109
	28	43.06	0.141
SCGC-2	3	40.47	0.123
	7	43.20	0.155
	28	46.55	0.137
OPC Control Mix	3	23.44	0.162
	7	31.90	0.146
	28	41.02	0.176

4.9 Creep

The creep and drying shrinkage behaviour of fly ash-based SCGC was studied for a period of one year. Creep and drying shrinkage strains were measured for two SCGC mixtures (SCGC-1 and SCGC-2) and one OPC-based control mixture. The proportions of these mixtures and the details of creep test are given in Chapter 3. The creep and drying shrinkage tests commenced on the 7th day after casting the test specimens and the specimens for creep test were loaded at 40% of their compressive strength at the time of insertion into the creep frames.

Table 4.27 presents the applied sustained stress and the instantaneous strain measured immediately after the application of the sustained load. Using these data, the instantaneous elastic modulus was calculated. The values of instantaneous elastic modulus, given in Table 4.27 are almost similar to those found in the modulus of elasticity test for the present study.

Table 4.27 Instantaneous Strain and Instantaneous Elastic Modulus

Mix ID	7^{th} Day Compressive strength (MPa)	40% stress (MPa)	Elastic strain (με)	Instantaneous Elastic Modulus (GPa)
SCGC-1	39.84	15.94	798	19.975
SCGC-2	42.98	17.19	850	20.223
OPC Control	31.77	12.71	532	23.891

Figures 4.34 through 4.36 present the experimental total strain and drying shrinkage strain measurements for all three mixes. The complete creep test data for each of the mix investigated in the present study are given in Tables E.1 through E.3 in Appendix E. Each curve in the Figures 4.34 through 4.36 represents an average of the two measurements. The total strain was measured on the specimens in the creep test frame, while the drying shrinkage strain was obtained from the companion unloaded specimens.

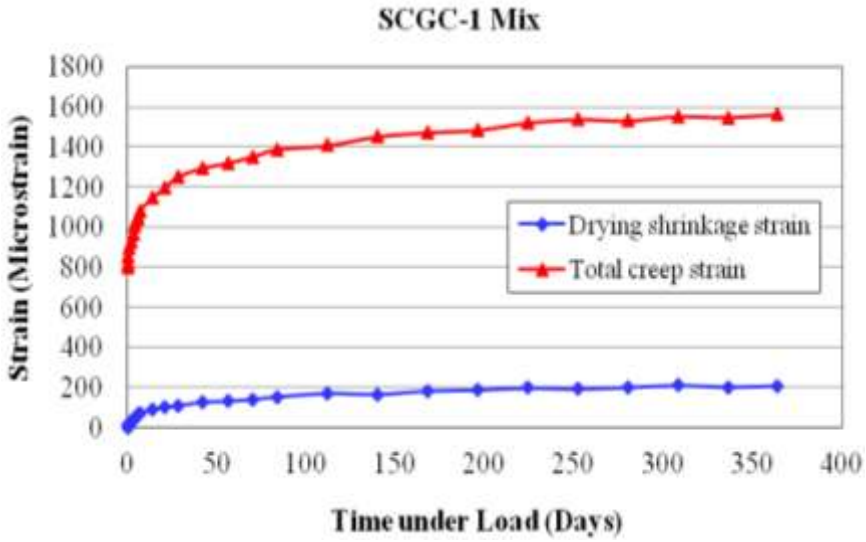

Figure 4.34 Total Creep and Drying shrinkage strian of SCGC-1 Mix

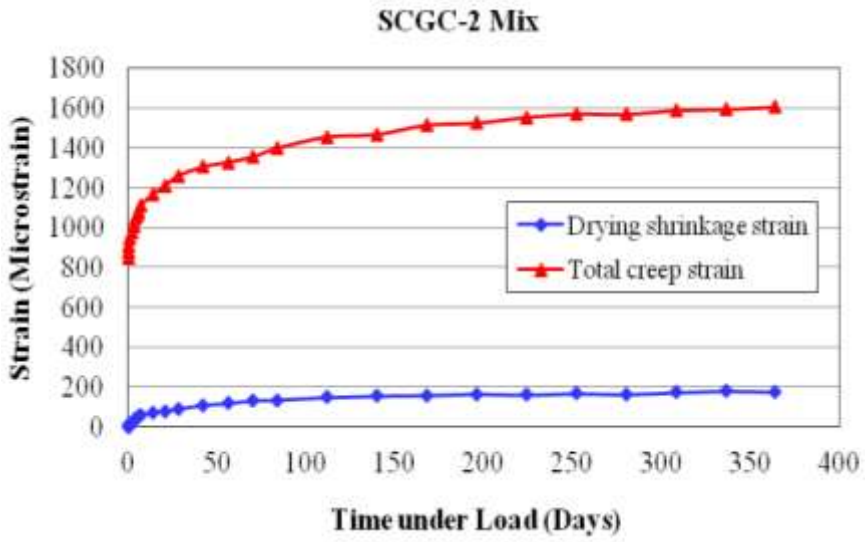

Figure 4.35 Total Creep and Drying shrinkage strian of SCGC-2 Mix

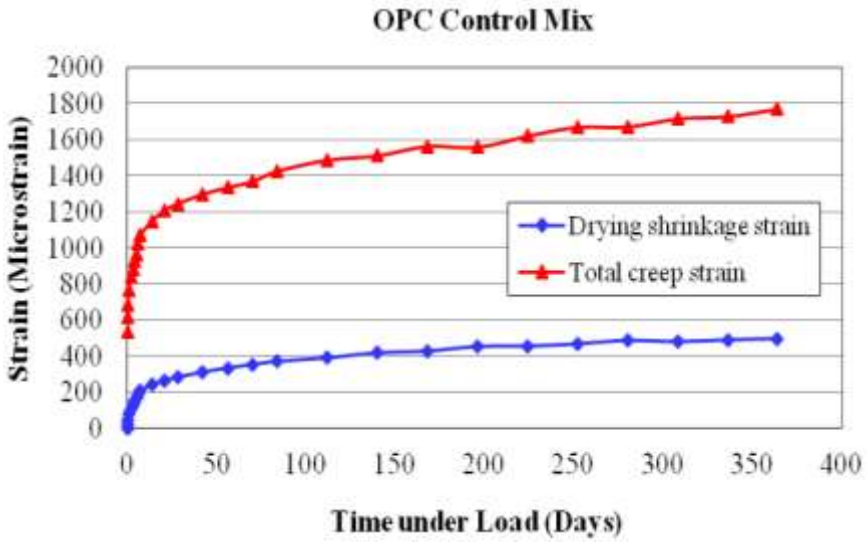

Figure 4.36 Total Creep and Drying shrinkage strian of OPC Control Mix

Creep strain data was obtained by subtracting the instantaneous elastic strain and drying shrinkage strain from the total strain. The creep strain data for Mixes SCGC-1, SCGC-2 and OPC control are presented in Figures 4.37 through 4.39.

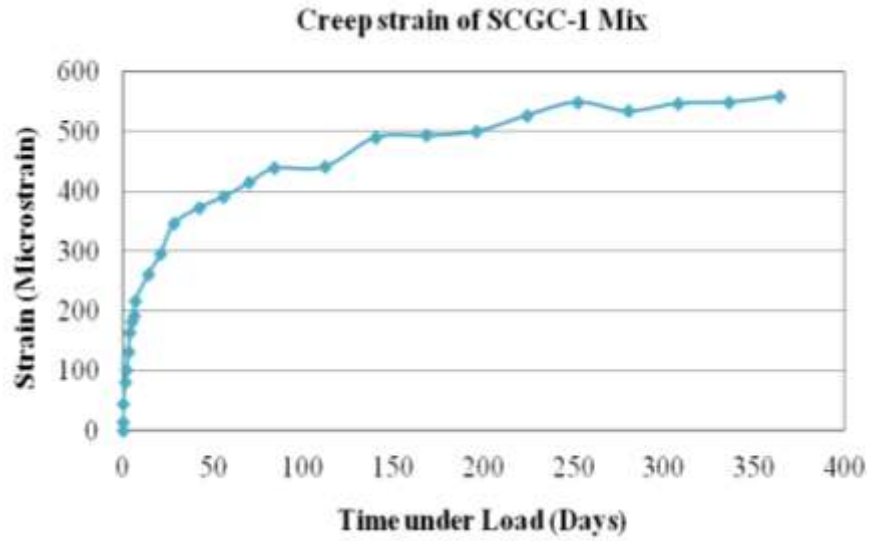

Figure 4.37 Creep strain of SCGC-1 Mix

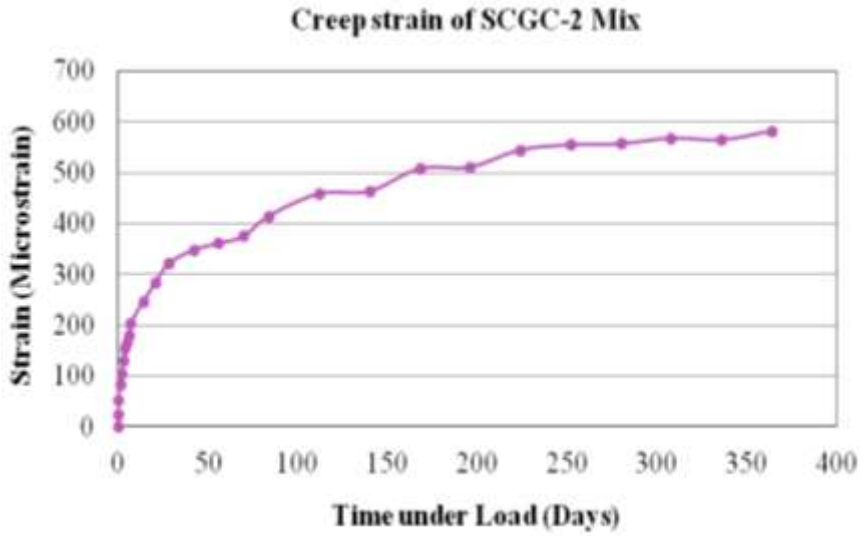

Figure 4.38 Creep strain of SCGC-2 Mix

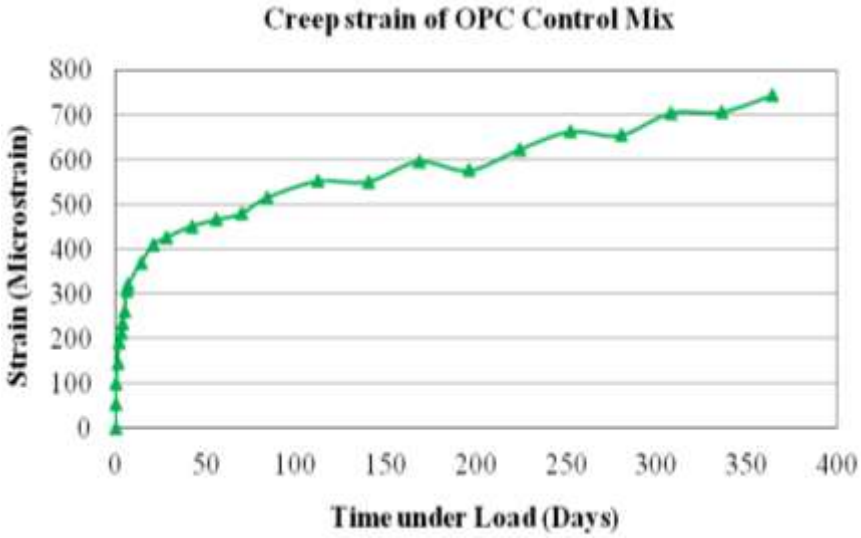

Figure 4.39 Creep strain of OPC Control Mix

Creep of concrete is normally described by either creep coefficient or specific creep. Specific creep, obtained by dividing the creep strain to the applied stress, is useful in comparing the creep behaviour of concretes of different compressive strengths. Creep coefficient, obtained by dividing the creep strain to the initial elastic strain, however gives better comparison to specific creep. As for creep coefficient, the effect of concrete stiffness is included by means of initial strain. Therefore, deformation results with the inclusion of elasticity factor for different concrete strength are more consistent as compared to specific creep [38]. For the present study, however both specific creep and creep coefficient were calculated. The values of

creep coefficient and specific creep for all the three mixes after one year of loading are summarised in Table 4.28 and shown in Figures 4.40 to 4.47.

Table 4.28 Creep Coefficient and Specific Creep of SCGC and OPC Mix Concretes

Mix ID	7^{th} Day Compressive Strength (MPa)	After one year of Loading	
		Creep Coefficient	Specific Creep (με)/MPa
SCGC-1	39.84	0.7005	35.0690
SCGC-2	42.98	0.6835	33.7987
OPC Control	31.77	1.3985	58.5365

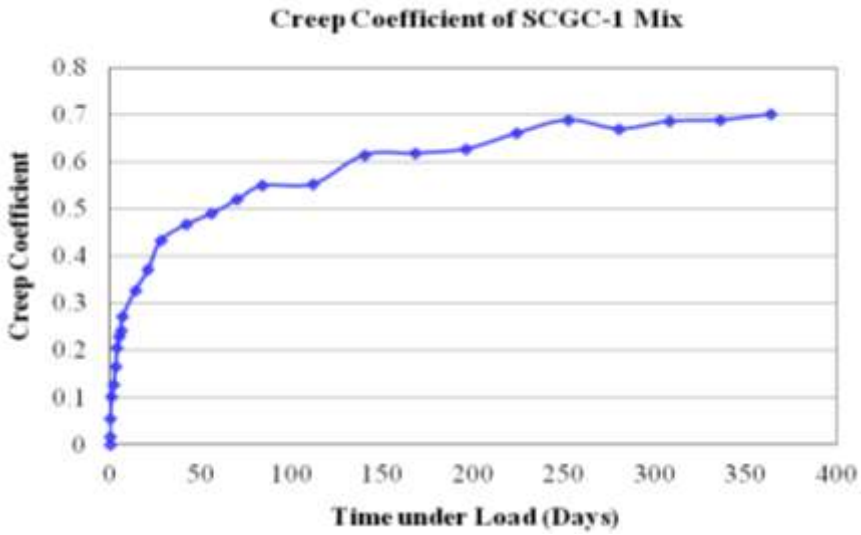

Figure 4.40 Creep Coefficient of SCGC-1 Mix

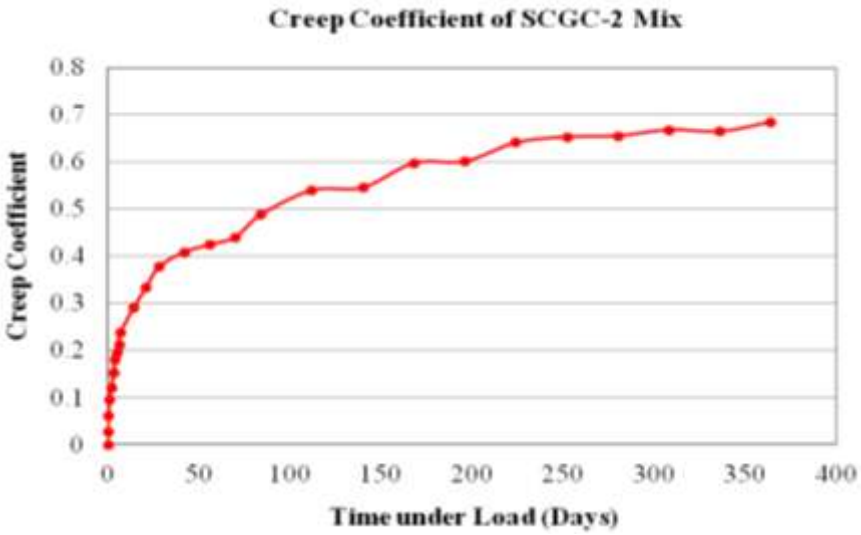

Figure 4.41 Creep Coefficient of SCGC-2 Mix

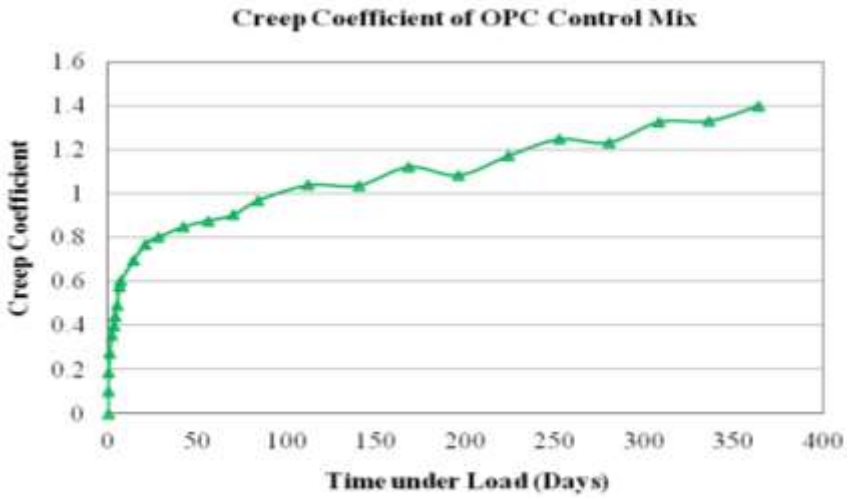

Figure 4.42 Creep Coefficient of OPC Control Mix

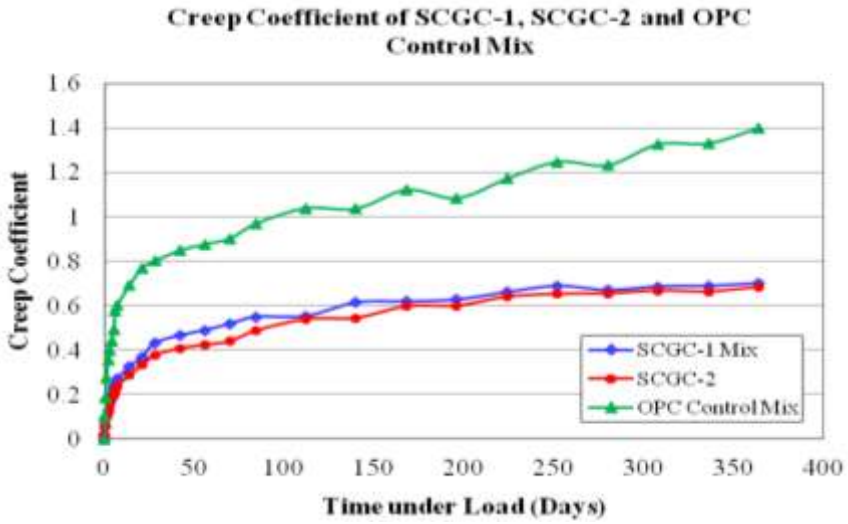

Figure 4.43 Creep Coefficient of SCGC and OPC Control Mixes

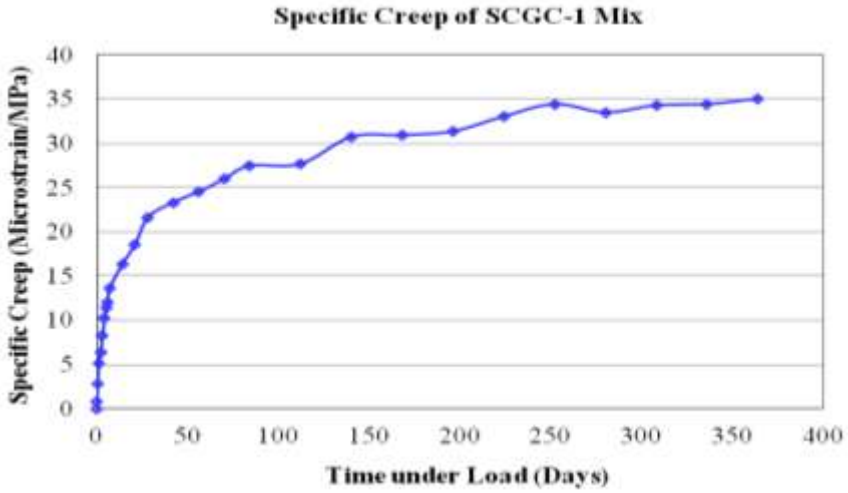

Figure 4.44 Specific Creep of SCGC-1 Mix

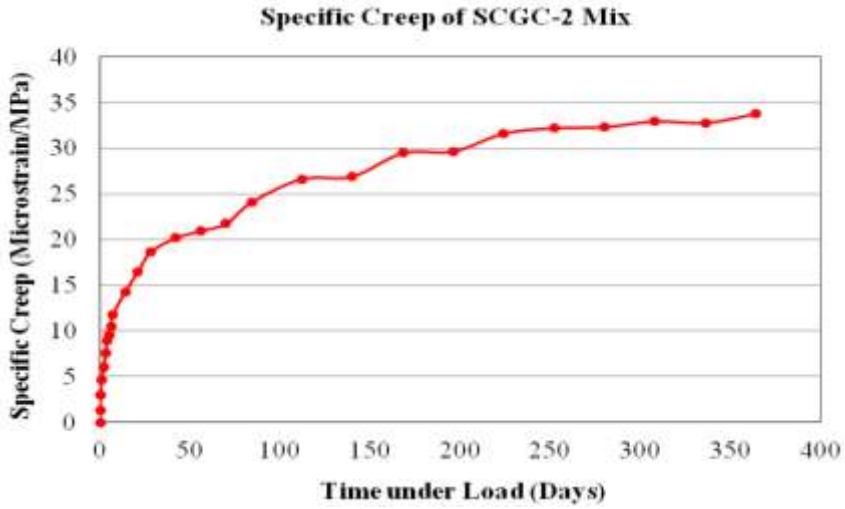

Figure 4.45 Specific Creep of SCGC-2 Mix

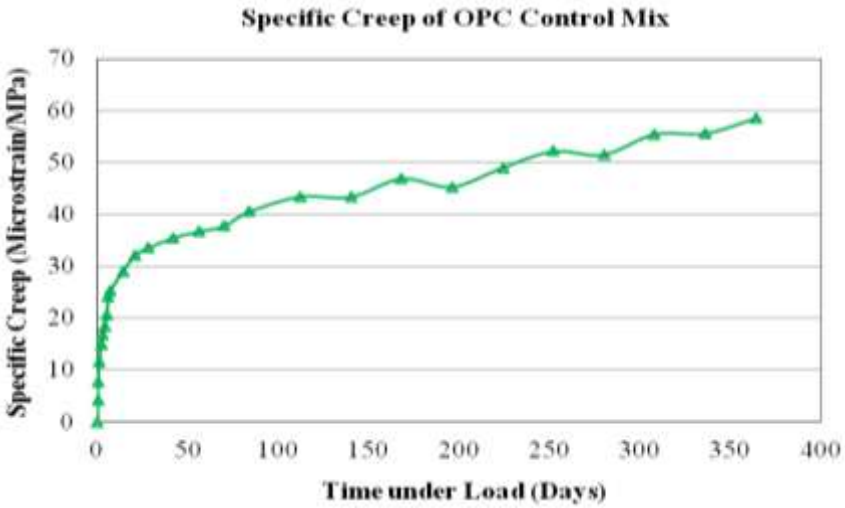

Figure 4.46 Specific Creep of OPC Control Mix

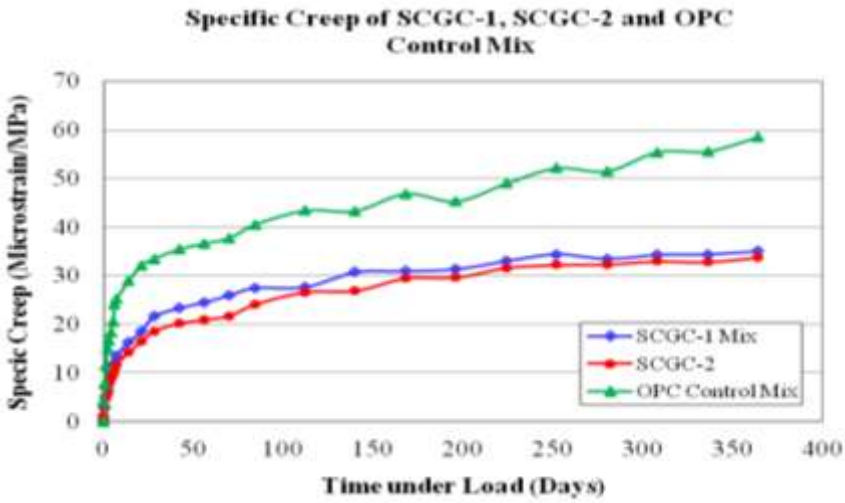

Figure 4.47 Specific Creep of SCGC and OPC Control Mixes

The test results generally indicate that fly ash-based SCGC undergoes lesser creep compared to Portland cement concrete. Test results, as presented in Table 4.28 and Figures 4.40 to 4.47, show that the creep coefficient and specific creep of both SCGC mixes are well below to the corresponding values of OPC control mix. For heat-cured fly ash-based SCGC with compressive strength of 40 and 43 MPa, the creep coefficient after one year of loading is around 0.68 to 0.70, while the specific creep is about 33.80 to 35.07 με/MPa. These values are about 50-60% of those experienced by OPC-based concrete. This may be due to restraining effects of unreacted fly ash residue particles acting as micro aggregates in geopolymer-based concretes as claimed by Wallah and Rangan [13]. In fly ash-based geopolymer concrete, during geopolymerization, the fly ash particles are not completely dissolved by the alkaline solution and the polymerization process that takes only on the surface forms the blocks necessary to produce the geopolymer binder. Thus, the unreacted fly ash residue particles are not destroyed and remain stable so they can act as micro-aggregates in the system and could increase the content of aggregate in concrete.

It is known that creep of concrete is affected by several factors including water and cement content, water-cement ratio, aggregate content and characteristics, cement composition, mix proportions, curing and storage conditions, age at time of loading, duration and magnitude of the loading, and size of the specimen. Among all factors, the aggregate content has the most significant influence on creep of concrete [37, 72]. The creep of concrete will decrease with the increase in the quantity of aggregates. For the present study, though, the same proportion of aggregates was used in the formulation of SCGC and OPC mixtures. However, the presence of 'micro-aggregates' due to the 'block-polymerization' concept as mentioned above might increased the restraining effect of fly ash-based SCGC mixes resulting in smaller creep compared to OPC-based concrete.

The results obtained from the current study are in good agreement with the results reported by other researches [13, 71] on fly ash-based geopolymer concrete. After one year of loading, Wallah and Rangan [13] obtained creep coefficient values between 0.4 and 0.7 for compressive strengths of 40 to 67 MPa while the specific creep ranged from 15 to 29 με/MPa for the corresponding compressive strength of 67 MPa to 40 MPa. Similarly, in a recent study on creep and drying shrinkage behaviour of fly ash-

based geopolymer concrete, Sagoe-Crentsil et al. [71] reported that the creep coefficient after one year of loading for the steam-cured geopolymer concrete with compressive strength of 40 MPa was of the order of 0.10. This value was about 40-60% lower than the corresponding OPC-based concrete.

4.10 Drying Shrinkage

The drying shrinkage strains for the three concrete mixes (SCGC-1, SCGC-2 and OPC Control) are presented in Figures 4.48 through 4.51. The proportions of these mixtures and the details of drying shrinkage test are given in Chapter 3. Complete drying shrinkage test data for each of the mix are given in Tables F.1 through F.3 in Appendix F. Test results indicate that heat-cured fly ash-based SCGC undergoes very low drying shrinkage compared to OPC concrete. It can be seen that the drying shrinkage strains of the OPC control mixture specimens cured in water are many folds larger than those experienced by the heat-cured SCGC mix specimens. As expected the shrinkage strain increased with the time of exposure. After one year of exposure, the drying shrinkage strains of fly ash-based SCGC mix specimens ranged between 141 and 159 microstrains compared to the value of 466 microstrains, experienced by control OPC mix specimens. These values are about 65-70% lower than that of OPC concrete. This may be due to the less amount of water present in the micro-pores of the hardened SCGC [13]. As, in heat-cured geopolymer-based concretes, most of the water is released during the geopolymerization process and evaporate during the curing process consequently reducing the drying shrinkage [1]. The lower drying shrinkage values obtained for SCGC mixes may also be partly due to a finer disconnected capillary network structure [71]. It is believed that the increased condensation processes occurring in heat-cured geopolymer-based concretes might have implications on the shrinkage process. Thus, when the condensation reaction of geopolymer concretes are accelerated by heat curing, the associated initial drying shrinkage is significantly reduced, signifying the completion of initial condensation reaction and the moisture loss from capillaries, as also verified by the associated rapid strength development [71].

The values of drying shrinkage strains for fly ash-based SCGC obtained in this study are in agreement with the results reported by other researchers [13, 71]. Wallah and Rangan [13] reported that after one year of exposure, the drying shrinkage strain values for heat-cured fly ash-based geopolymer concrete with compressive strengths of 41 to 65 MPa were around 100 microstrains. Similarly, Sagoe-Crentsil et al. [71] in their study on creep and drying shrinkage performance of geopolymer concrete reported that the shrinkage values of steam-cured fly ash-based geopolymer concrete fell well below the nominal 700 microstrain limit, with geopolymer concrete values typically less than 400 microstrain after one year.

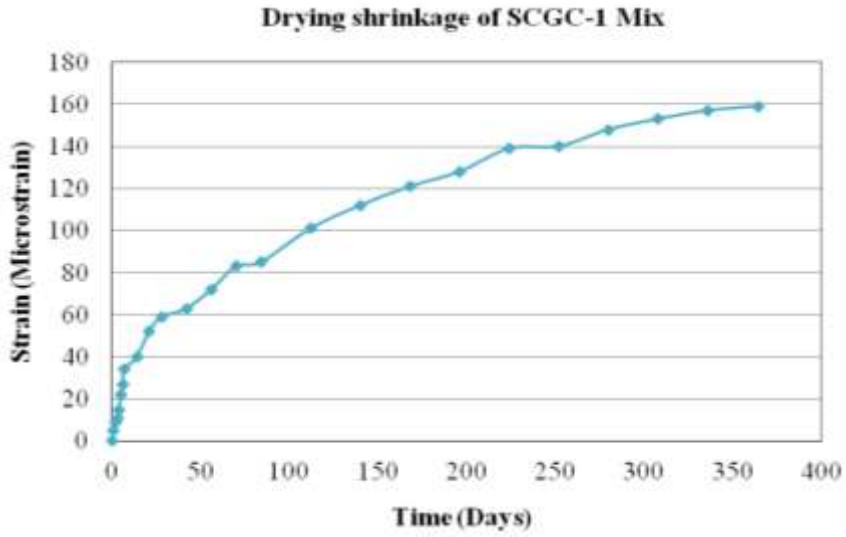

Figure 4.48 Drying shrinkage of SCGC-1 Mix

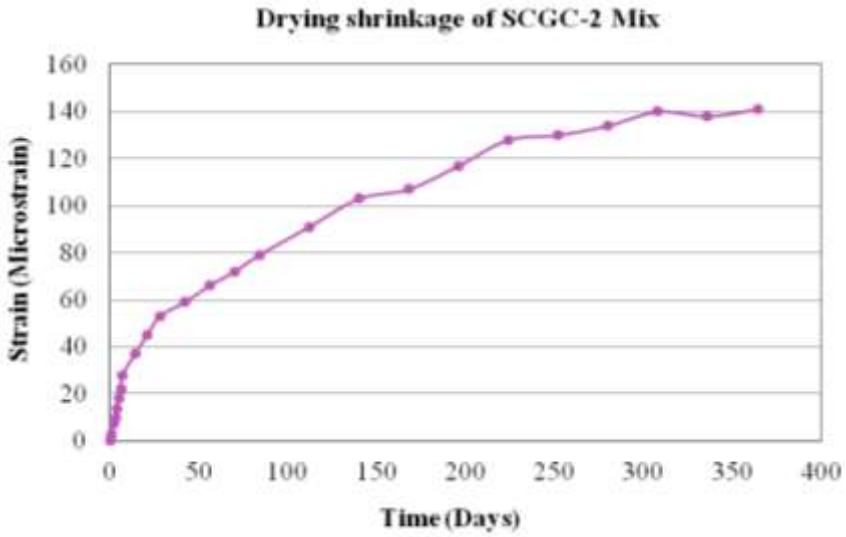

Figure 4.49 Drying shrinkage of SCGC-2 Mix

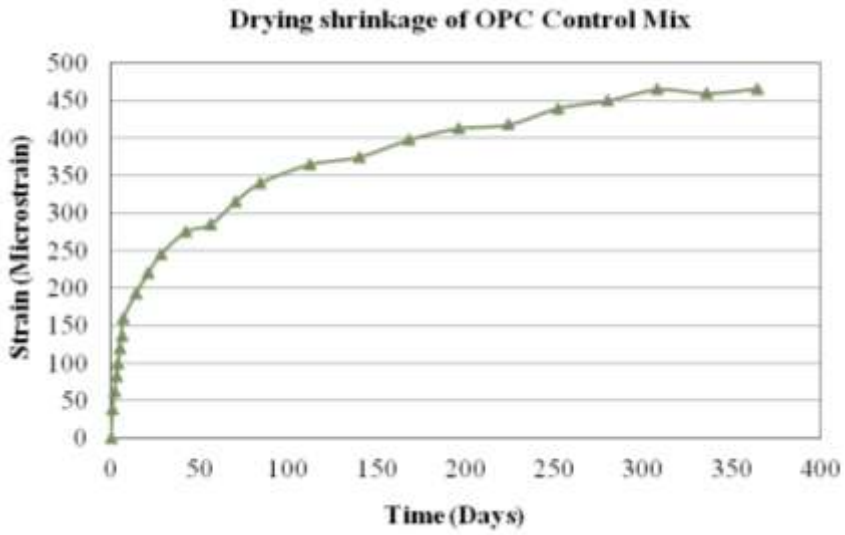

Figure 4.50 Drying shrinkage of OPC Control Mix

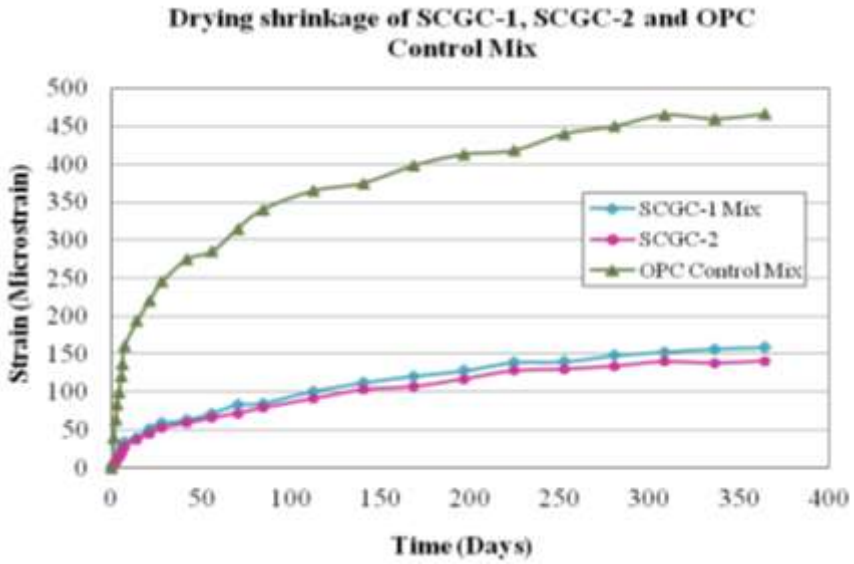

Figure 4.51 Drying shrinkage of SCGC and OPC Control Mixes